This paper should be cited at:
Sharifzadeh M*, Wang L., Shah N., (2015). Decarbonisation of olefin processes using biomass pyrolysis oil. *Applied Energy*, 149, 404–414, (Link).

Decarbonisation of Olefin Processes using Biomass Pyrolysis Oil

Sharifzadeh M [a]*[1], Wang L[b] and Shah N [a]

[a] Centre for Process Systems Engineering (CPSE), Department of Chemical Engineering, Imperial College London. [b] Centre for Environmental Policy, Imperial College London.

An imperative step toward decarbonisation of current industrial processes is to substitute their petroleum-derived feedstocks with biomass and biomass-derived feedstocks. For decarbonisation of the petrochemical industry, integrated catalytic processing of biomass pyrolysis oil (also known as bio-oil) is an enabling technology. This is because, under certain conditions, the reaction products form a mixture consisting of olefins and aromatics, which are very similar to the products of naphtha hydro-cracking in the conventional olefin processes. These synergies suggest that the catalytic bio-oil upgrading reactors can be seamlessly integrated to the subsequent separation network with minimal retrofitting costs. In addition, the integrated catalytic processing provides a high degree of flexibility for optimization of different products in response to market fluctuations. With the aim of assessing the techno-economic viability of this pathway, five scenarios in which different fractions of bio-oil (water soluble/ water insoluble) were processed with different degrees of hydrogenation were studied in the present research. The results showed that such a retrofit is not only economically viable, but also provides a high degree of flexibility to the process, and contributes to decarbonisation of olefin infrastructures. Up to 44% reductions in greenhouse gas emissions were observed in several scenarios. In addition, it was shown that hydrogen prices lower than 6 $/kg will result in bio-based chemicals which are cheaper than equivalent petrochemicals. Alternatively, for higher hydrogen prices, it is possible to reform the water insoluble phase of bio-oil and produce bio-based chemicals, cheaper than petrochemical equivalents.

Keywords: Decarbonisation, Olefins, Biomass Pyrolysis Oil, Techno-economics, Life Cycle Assessment.

[1] Corresponding author, E-mail: mahdi@imperial.ac.uk; Tel:+44(0)7517853422.

This paper should be cited at:
Sharifzadeh M*, Wang L., Shah N., (2015). Decarbonisation of olefin processes using biomass pyrolysis oil. *Applied Energy*, 149, 404–414, (Link).

1. Introduction

Amongst major energy-users and GHG emitters, industrial processes are responsible for one third of the total worldwide energy consumptions and associated emissions. In addition, many industrial processes consume energy products as their feedstock. The main challenge is that industrial processes have long life cycles, in the order of decades, and the number of new processes which are being built is significantly smaller than the number of processes which are currently in use. These observations suggest that an important pathway toward decarbonisation of industrial processes is through retrofitting these processes. In particular, substituting petroleum-derived feedstocks with renewable feedstocks has substantial potential for mitigating the greenhouse gas (GHG) emissions and protecting the environment. However, most of the research in the field is focused on developing new processes which are subject to a high degree of uncertainty in sale-up and commercialization. The present paper explores the opportunity for substituting the naphtha feedstock in a conventional olefin process with biomass pyrolysis oil (also known as bio-oil). The research significance is due to the fact that the olefin process is highly energy-intensive and its products are essential for polymer production. Therefore, alternative production pathways have been under scrutiny [1-5].

The pathways for producing liquid fuels from biomass include fractionation, liquefaction, pyrolysis, hydrolysis, fermentation, and gasification [6], among which biomass pyrolysis provides the cheapest pathway toward renewable chemicals and fuel [7]. In principle, pyrolysis is the precursor of biomass gasification or combustion and refers to set of reactions occurring when biomass is heated in the absence of oxygen [6]. Nevertheless our knowledge of biomass pyrolysis is limited; Mettler, *et al*., [8] identified ten fundamental challenges in biomass pyrolysis with an emphasis on understanding the chemistry of conversion pathways, heat transfer phenomena and particle shrinkage. The diverse array of research into biomass pyrolysis include advanced analytical chemistry methods for bio-oil characterization [9-11], developing kinetic models for the pyrolysis reactions [12], computational fluid dynamic studies [13], design of new reactors [14], developing new heating methods such as microwave assisted pyrolysis [15,16], optimizing the bio-oil yield and process configuration [17], developing various bio-oil upgrading methods [18], process intensification [19], techno-economic analysis [20,21] , environmental assessment [22], and enterprise-wide and supply chain optimization [23-25]. A recent review of the research into biomass fast pyrolysis has been published by Meier *et al*., [26].

Despite various economic incentives, biofuel commercialization poses an important challenge; the effluent of pyrolysis reactions, called bio-oil features undesirable properties such as chemical instability, high acidity, low heating value and immiscibility with petroleum-derived fuels. Therefore,

upgrading bio-oil poses an important challenge. The conventional technologies for upgrading bio-oil include aqueous processing, hydrodeoxygenation (HYD), and zeolite cracking. The most common upgrading method is hydrotreatment upgrading of bio-oil which was originally inspired by similar processes for hydrodesulfurization (HDS) and hydrodenitrogenation (HDN) in petroleum refineries [27]. However, the amount of heteroatoms (*i.e.*, oxygen) is an order of magnitude larger in the case of bio-oil. The implication of high oxygen content is excess coke formation. The resolution is multistage treatment in which firstly the bio-oil is stabilized in a low temperature reactor and then a deeper hydrodeoxygenation is accomplished in the second stage reactor at a higher temperature [28]. Here, we differentiate between *char* and *coke*. The former is a by-product of biomass pyrolysis, and is favored at relatively low temperature and low heating rate [29]. By contrast, the latter refers to the carbon atoms deposited on the catalysts surface of the upgrading reactors and is favored at low hydrogen partial pressures, [7, 30].

While hydrotreating does not alter the boiling range of hydrocarbons significantly, zeolite cracking is an efficient pathway to produce large qualities of light products by depolymerisation of heavy oligomers [31]. The challenge is that the coking can be so severe that a fixed bed reactor may become plugged quickly. Pretreatment using multi-stage hydrodeoxygenation can mitigate the problem [32]. In addition, fluidized bed reactors have the advantage that the coked catalyst can be regenerated and recycled to the reactor. Aqueous processing (also known as hydrothermal treatment) refers to a water-rich scenario at temperature above 200^{o}C, and a pressure sufficiently high to maintain the water at the near supercritical or supercritical state. It is widely observed that at these conditions water exhibits distinct processing advantages such as enhanced and tunable properties (*e.g.* solubility, solvent polarity, transport properties), and ease of solvent removal [33]. Other advantages of this technology include avoiding phase change and parasitic energy losses due to high pressure processing, versatile chemistry to existing chemical and fuel infrastructure, enhanced reaction rates [34], and minimal hydrogen consumption [35]. However, the engineering challenges include unknown reaction mechanisms, uncharacterized reaction pathways and severe processing conditions that the catalysts may not withstand.

Techno-economic performance of the fast pyrolysis pathway has been the focus of intensive research. Initial evaluations were made by research institutes. For example a detailed techno-economic analysis was conducted by Jones et al., [36] at Pacific North West National Laboratory (PNNL). The process consisted of a circulating fluidized bed pyrolysis reactor followed by two-stage hydrogenation reactors. Then, in a sequence of distillation columns, the stabilized bio-oil was resolved into biofuels with similar properties to naphtha and diesel. The heavy fraction was sent to a

hydrocracker before recycling to the distillation columns. In this process, the hydrogen required for bio-oil hydrogenation and hydrocracking was produced through reforming natural gas. A technoeconomic comparison was made to the scenario where the process was co-located with a conventional refinery and the hydrogen was imported. Since the economy of bio-oil production is a strong function of hydrogen prices, Wright et al., [37] proposed a process in which, a fraction of bio-oil was partially reformed to produce the required hydrogen for upgrading the remaining bio-oil. They concluded that producing hydrogen from bio-oil itself is more profitable compared to purchasing hydrogen. Recently, Shemfe, et al., [38] studied the technoeconomic performance of fast pyrolysis for cogeneration of biofuel and electricity power. A merit of this study was incorporation of rate-based chemical reactions for modelling the hydroprocessing section. In parallel, technoeconomic analysis of producing commodity products through catalytic upgrading the bio-oil has been the focus of several researchers. Vispute, et al., [7] showed that the annual economic potential (EP) of this pathway strongly depends on the hydrogen price. Later, Brown, et al., [39] conducted a more detailed techno-economic analysis. They identified the biomass pyrolysis yield as an important factor in economic viability of this technology. Later, Zhang et al., [40] compared the biofuel pathway with the commodity chemical pathway. They concluded that a scenario where the required hydrogen is produced through natural gas reforming is the most economic option. All the aforementioned studies applied simplified process flowsheeting sufficient for calculating overall mass balances and did not include the sophisticated separation network required for resolving the highly complex olefin-aromatic mixture into marketable high purity products. The present research extends the previous studies by adapting the catalytic upgrading technology for retrofitting existing olefin process and evaluates the opportunity for decarbonisation of olefin industries through substitution of their conventional petroleum feedstocks (e.g., naphtha) using the renewable pyrolysis bio-oil. The present analysis is comprehensive and includes technoeconomic as well as environmental life cycle assessments.

Recently, Vispute, *et. al*, [7] developed a reaction network for upgrading bio-oil which combines the advantages of all three aforementioned technologies in order to produce an array of olefin and aromatic products as a fungible feedstocks for existing refinery and petrochemical infrastructure. In their proposed reaction network, firstly the thermal stability and hydrogen content of the bio-oil is improved and then using a suitable zeolite catalyst with the desirable pore size and active sites, it is converted to primary olefins and aromatic products. Another advantage of this methodology is that due to thermal stabilization and hydrogenation at low temperatures, coke generation is minimized and the overall carbon efficiency is as high as 60%. In addition, the multi-stage processing provides a

high degree of flexibility to optimize the yield of products. In their proposed scheme, the reaction network consists of three reactors which provide alternative routes for upgrading and enables optimization of the product properties and carbon yields as well as the hydrogen consumption. Firstly, the crude bio-oil is mixed with water at a mass ratio of four units of water per a unit of the crude-bio-oil. Then, the mixture is phase separated in a decanter. The aqueous phase, also called water soluble bio-oil (WSBO), is sent to a low-temperature hydro-processing unit which operates at 398 K and 100 bar. This is the highest temperature with no risk of catalyst coking and reactor plugging. Supported Ru was identified as the most active and selective catalyst for aqueous phase hydro-processing. The partially stabilized bio-oil is then fed to the second hydrogenation stage which operates at 523 K and 100 bar. Supported Pt was identified as the best catalyst for this stage with desirable properties such as high C-O hydrogenation and low C-C bond cleavage activities. The third reactor provides an upgrading step over the zeolite catalyst in order to produce olefins and aromatics. Vispute *et. al*., [7] demonstrated that the overall yields of the aromatic and olefin products depends on the extents of the added hydrogen in the first two stages and therefore the reaction network will provide the option for optimization of the products yields. In the present research, similar to Vispute, *et. al*, [7], five scenarios were studied and compared:

Scenario (1): the whole bio-oil (WSBO+WIBO) is directly sent to the zeolite upgrading stage;

Scenario (2): the whole bio-oil (WSBO+WIBO) is firstly hydrotreated in a low temperature reactor and then processed in the zeolite upgrading reactor;

Scenario (3: water soluble bio-oil (WSBO) is sent directly to the zeolite upgrading stage;

Scenario (4): water soluble bio-oil (WSBO) is firstly hydrotreated in a low temperature reactor and then processed in the zeolite upgrading reactor;

Scenario (5): only water soluble bio-oil (WSBO) is processed in all the three hydrotreating and upgrading reactors.

In scenarios 3-5, the water insoluble bio-oil (WIBO) is sold as a low quality fuel product (half of the coal price [39]). However, considering the sensitivity of the process to the hydrogen price, an additional scenario was studied, which is equivalent to the fifth scenario but the water insoluble bio-oil is reformed to produce the required hydrogen. The remaining sections of this paper are organized as follows. Firstly the synergies and integration opportunities between the integrated catalytic process of bio-oil and the conventional olefin processes are discussed. The next section will evaluate the flexibility of integrated catalytic processing in optimizing the yields of various products. These discussions will enable proposing the bio-oil as a substitute feedstock for existing olefin

infrastructures. The rest of the paper will focus on the evaluating alternative process configurations for integrated catalytic processing of bio-oil with respect to economic and environmental measures. Finally the paper will conclude with discussions and suggestions for future research. It is notable that the detailed process flow diagrams and experimental data used for process modelling are summarized in the enclosed Electronic Supplementary Materials (ESM).

2. Methodology and approach

The following sections report the methods employed for process design, economic evaluation and life cycle analysis. The features of interest are adapting the process configuration to the new biomass-derived feedstock, evaluating process flexibility, the applied approach for economic analysis and the method for the environmental impact assessments.

2.1. Retrofitting existing olefin processes for biomass feedstock

The products of integrated catalytic processing of pyrolysis bio-oil are a mixture consisting of olefins and aromatics, which is very similar to the effluent of naphtha hydro-cracking in the conventional olefin processes. Similarities and differences between the effluents of the bio-oil upgrading process and the effluents of naphtha hydrocracking are shown in Table 1. This table reveals an important difference; the bio-oil pathway produces significantly larger amount of carbon dioxide compared to the naphtha pathway. This is the implication of biomass chemistry. For example, hybrid poplar has more than 41% (mass basis) oxygen content [41] and the carbon oxides are produced from oxygenates through upgrading reactions. Table 1 also suggests that the two processes have eleven common components from which seven components are the main products of both processes. However, the conventional naphtha hydrocracking process produces a minor fraction of olefins with higher (≥3) number of unsaturated bonds. These highly active components conventionally are not separated, but saturated in hot and cold sections. The following subsections examine if an existing olefin process can be retrofitted to substitute naphtha by bio-oil.

The block diagram of a conventional olefin process is shown in Fig. 1.a. The process consists of three main sections: hot section, cold section, and pyrolysis gasoline hydrogenation (PGH) section. In the hot section, the naphtha feedstock is mixed with water and fed to high temperature reactors (several parallel furnaces) where it is converted to a mixture of olefins, aromatics and heavy components, called *Cracked Gas* (Tables 1). This mixture is quickly quenched and the large amount of inert water and heavy hydrocarbons are separated using distillation columns. The water is stripped from light gases and recycled to the furnaces. The cleaned cracked gas is sent to an energy induced separation network, comprising a large-scale multi-stage compressor and a stripper [42].

The aim of cracked gas compression is to elevate the required temperatures for cryogenic distillation of light products. The compressed mixture of olefin products is dried and sent to a cryogenic distillation train (*i.e.*, cold section) where it is resolved to pure components. In parallel, as a result of sequential compression and cooling of the cracked gas, most of the aromatic components condense which after stripping the dissolved gases, are sent to the PGH section. The aromatic mixture has properties very similar to gasoline. However, it also contains highly reactive dissolved olefins which if stored unsaturated, will result in polymerization and degradation of the gasoline. Therefore, the aromatic mixture is firstly saturated using hydrogenation reactors and then sent to a distillation train where it is resolved to various hydrocarbon cuts. A more detailed description of the naphtha-based olefin process can be found in the literature [43].

Fig. 1.b shows the retrofitted process including the additional processing steps. Biomass is firstly sent to the pyrolysis section where it is converted to light gases, condensable hydrocarbons and coke. Unfortunately, the hydrocarbon condensates, called bio-oil, suffer from some undesirable properties such as high oxygen content, low energy content and immiscibility with petroleum-derived fuels. Therefore, the bio-oil product is sent to the next section for upgrading. As discussed earlier, this section consists of three reactors, a low temperature hydrogenation reactor, a high temperature hydrogenation reactor, and a zeolite upgrading reactor. The effluent of this section is a highly complex mixture of carbon oxides, water, olefins and aromatics, which is sent to separation sections. The aforementioned similarities between the effluents of the integrated upgrading process and the naphtha-derived cracked gas suggest that the separation sections 300-600 are very similar. More details of the retrofitted process including process flow diagrams and detailed process description are presented in the Electronic Supplementary Material (ESM).

This paper should be cited at:
Sharifzadeh M*, Wang L., Shah N., (2015). Decarbonisation of olefin processes using biomass pyrolysis oil. *Applied Energy*, 149, 404–414, (Link).

215 **Table 1. Comparison between the effluents of naphtha hydrocracking (Cracked Gas) and integrated**
216 **upgrading of bio-oil (Scenario 5) – mass fraction (dry basis).**

	Cracked Gas [42]	Scenario 5 [7]
Hydrogen	0.0115	
Cox	**0.0002**	**0.2351**
CO	0.0001	0.1010
CO_2	0.0001	0.1341
Coke		0.0941
H2S	0.0004	
C1 to C4 Alkanes	**0.2741**	**0.1406**
Methane	0.1738	0.0374
Ethane	0.0608	0.0351
Propane	0.0053	0.0343
Butane	0.0029	0.0339
Pentane	0.0261	
Hexane	0.0052	
Heptane	0.0005	
Olefins (double bonds)	**0.5069**	**0.3751**
Ethylene	0.3507	0.1200
Propylene	0.1277	0.2018
Butylene	0.0285	0.0533
Olefins (triple bonds)	**0.0601**	**0.0000**
Acetylene	0.0086	
13-Butadiene	0.0402	
Propadiene + M-Acetylene	0.0113	
C4 Acetylene	0.0020	
Aromatics	**0.1060**	**0.1481**
Benzene	0.0685	0.0400
Toluene	0.0208	0.0738
Styrene	0.0122	0.0019
Xylene + E-Benzene	0.0045	0.0323
Heavy Ends	**0.0382**	**0.0070**
C9-	0.0082	
C10+	0.0300	
Indene		0.0007
Naphthalene		0.0007
unidentified		0.0055

217
218

This paper should be cited at:
Sharifzadeh M*, Wang L., Shah N., (2015). Decarbonisation of olefin processes using biomass pyrolysis oil. *Applied Energy*, 149, 404–414, (Link).

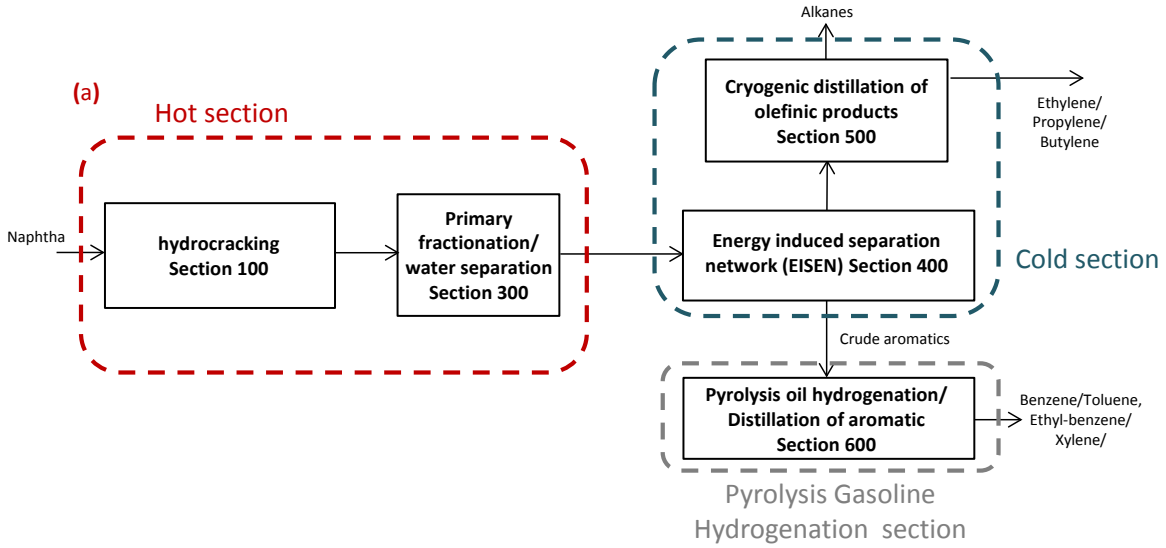

219

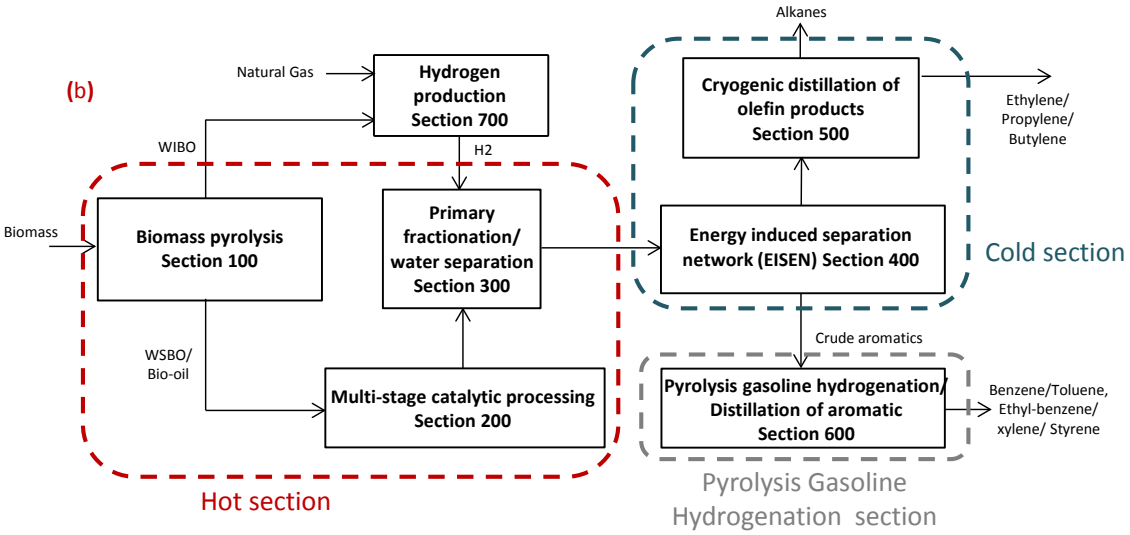

220
221 **Fig. 1. Process block diagrams for (a) conventional olefin process, (b) the retrofitted process using biomass**

222 There are three minor differences between the separation sections of process (a) and (b). Firstly, the
223 amount of carbon dioxide is larger in bio-mass derived bio-cracked gas. Therefore, the CO_2 scrubber
224 (see ESM for more details) should be retrofitted to handle larger amounts of CO_2. Secondly,
225 conventional cracking gas contains a fraction of olefins with a higher number of unsaturated bonds.
226 Due to the small amounts of these products they are often dealt as impurities and are saturated by
227 hydrogenation reactions. Since these components were not observed by Vispute *et. al.*, [7], the
228 corresponding equipment can be retired. Finally, the conventional cracked gas contains a large
229 amount of hydrogen which can be separated as a by-product in pressure swing adsorption (PSA)
230 columns. However, the biomass-based process is a net consumer of hydrogen due to the presence
231 of oxygenates.

This paper should be cited at:
Sharifzadeh M*, Wang L., Shah N., (2015). Decarbonisation of olefin processes using biomass pyrolysis oil. *Applied Energy*, 149, 404–414, (Link).

2.2. Process modelling

The process modelling was conducted using Aspen Plus™ simulator. The pyrolysis and upgrading reactors were modelled based on the yield data by Vispute, et. al., [7] and Jones, *et al*., [36]. High purity chemicals were produced (> 0.99 mass fraction). ENRTL-RK method described the thermodynamic properties. The simulation of pyrolysis section was validated using data from [36]. The model of the cryogenic section was validated using the data from Sharifzadeh *et al*.'s study [42]. The distillation columns were modelled using RADFRAC unit operation in Aspen Plus. The pressure swing adsorption was modelled using "SEP" unit operation in Aspen Plus, assuming 90% separation efficiency. The water soluble bio-oil fraction is reported to comprise 60-80% of the total oil, on the mass basis [44]. In the present study, the conservative value of 62% was adapted from [45].

Table 2. The modelling approach and operating conditions for major reactors.

Reactor	Description	T (K)	P (bara)	Modelling approach	Ref.
R101 (Fig S1) [a]	Pyrolysis reactor	773	1.08	Yield	[36]
R201 (Fig S2) [a]	Low temperature hydrogenation reactor	398	100	Yield	[7]
R202 (Fig S2) [a]	High temperature hydrogenation reactor	523	100	Yield	[7]
R203 (Fig S2) [a]	Zeolite cracking reactor	873	1.01	Yield	[7]
R601 (Fig S5) [a]	Pyrolysis gasoline hydrogenation reactor	433	27	Conversion (100% olefins)	-
R701 (Fig S6) [a]	Reformer reactor	1123	25.8	Chemical Equilibrium	[36]
R-702 (Fig S6) [a]	High temperature gas shift reactor	626	24.8	Conversion (80% CO)	[36]

(a) Please refer to the Electronic Supplementary Material (ESM) for the process flow diagrams, Figs. S1,S2,S5,S6.

Table 2 reports the modelling approach and operating conditions applied for simulating the main reactors. The pyrolysis reactor was modelled using the yield data from a previous study by DOE [36]. The compositions and flowrates of the pyrolysis reactor feed and products are shown in Table S4-ESM. The integrated catalytic reactors were modelled using the experimental yield data from Vispute *et al*.'s study [7]. The elemental analysis used for modelling water soluble bio-oil (WSBO) and water insoluble bio-oil (WIBO) were from [45] and are shown in Table S5. The product compositions of the low temperature hydrogenation reactor (R-201 in Fig S2) and the high temperature hydrogenation reactor (R-202 in Fig S2) are shown in Table S5-ESM. Table S1 shows the product compositions and flowrates of the zeolite cracking reactor (R-203 in Fig S2-ESM) in different scenarios (1-5), adapted from [7]. The experimental results from [7] were reported in terms of identified carbon contents and were converted to mass and mole fractions using molecular weight and molecular formula of each component. Table S1-ESM reports the amount of required hydrogen in each Scenario (1-5), [7]. The pyrolysis gasoline hydrogenation reactor was modelled based on

100% conversion of olefins. The required amount of hydrogen was calculated based on the amount unsaturated carbon in the reactor feed. The reformer (R-601 in Figure S5-ESM) was modelled based on chemical equilibrium using Gibbs free energy minimization [49]. The high temperature gas shift reactor was modelled based on 80% of conversion of CO though water gas shift reaction [36]. The costs of conventional unit operations (*e.g.*, distillations, compressors) were evaluated using Aspen Economic Analyzer™. The costs of nonconventional unit operations (*e.g.*, reformer, pyrolyzer) were calculated by scaling with respect to economic data from [36].

2.3. Process flexibility

Another key feature of process design and retrofitting is to ensure flexibility of the process in response to fluctuation in the demand and the prices of products. In the present research, a yield-based optimization was formulated to study different scenarios in which the carbon content of each product stream is maximized. To this end, the superstructure of the integrated upgrading reactors was constructed, as shown in Fig. 2. Table 3 suggests that by adjusting Valves 201-205, it is possible to optimize the amount of feed to each reactor, and hence the product yields. For example, the configuration in which Valve 201 is open and other valves are closed corresponds to Scenario (1). The arrangements of valves are similar in Scenarios 5 and 5 w/ reformer. The difference is that in Scenario 5 w/ reformer, water insoluble bio-oil is used for hydrogen production, but in Scenario 5, it is sold.

Fig. 3 shows the results of flexibility optimization. This figure suggests that the process can be optimized toward generation of various products with a high degree of flexibility. For example, Scenario 5 is well posed to maximize the yield of olefin products. However, Scenario 2 is more appropriate for producing aromatics. By comparison, Scenario 1 produces heavier products. In practice, the designer may desire to include all the three reactors and oversized them so the yields of different products can be optimized in real-time. An interesting observation was that the optimizer chose between Scenarios (1-5) and not a combination of them, implying that the reactor temperatures (hence the product yields) are well posed for optimizing different product cuts.

Table 3. The position of valves in Fig. 2 for different upgrading scenarios

	SC1[(a)]	SC 2	SC 3	SC 4	SC 5	SC 5 w/ reformer
Valve-201	Open	Open	Close	Close	Close	Close
Valve-202	Close	Close	Open	Open	Open	Open
Valve-203	Close	Open	Close	Open	Open	Open
Valve-204	Close	Close	Close	Close	Open	Open
Valve-205	Close	Close	Close	Open	Close	Close

(a) SC1 refers to Scenario 1

This paper should be cited at:
Sharifzadeh M*, Wang L., Shah N., (2015). Decarbonisation of olefin processes using biomass pyrolysis oil. *Applied Energy*, 149, 404–414, (Link).

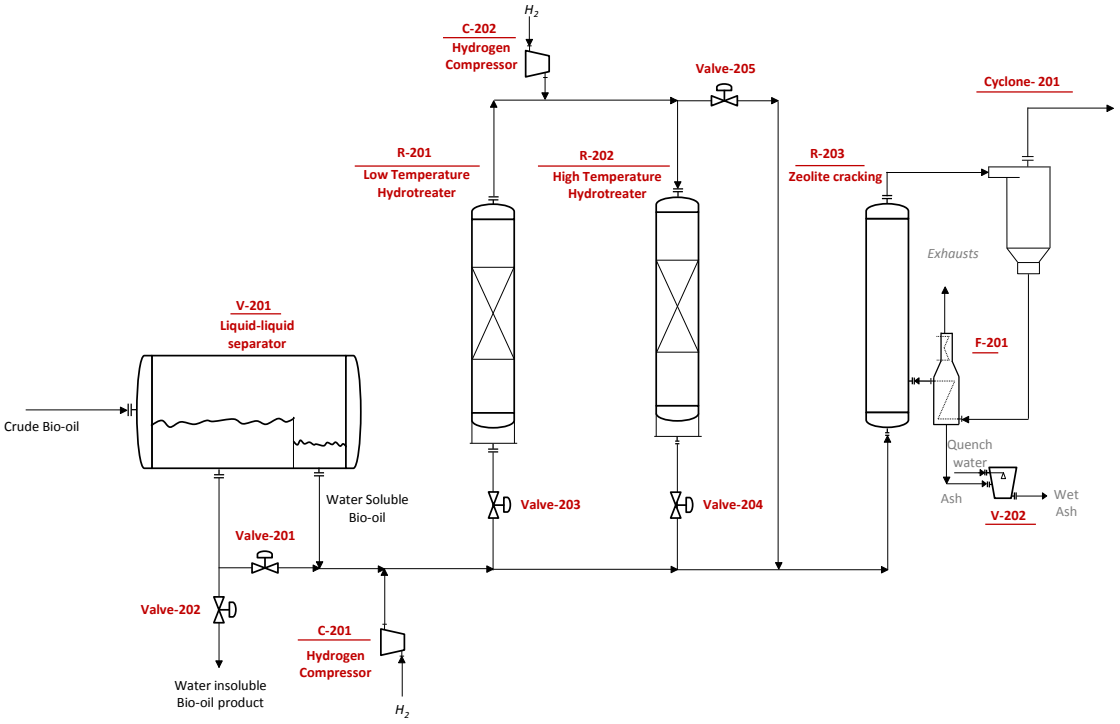

285

286 **Fig. 2. Integrated catalytic upgrading of bio-oil: adjusting Valves 201-204 allows optimization of the product**
287 **yields**

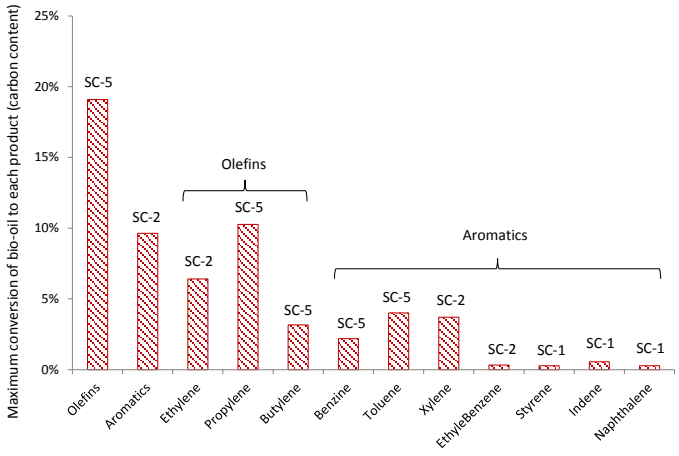

288

289 **Fig. 3. The result of flexibility optimization: the maximum carbon conversion to each product**

This paper should be cited at:
Sharifzadeh M*, Wang L., Shah N., (2015). Decarbonisation of olefin processes using biomass pyrolysis oil. *Applied Energy*, 149, 404–414, (Link).

2.4. Economic evaluation

2.4.1. Cost estimation

It is assumed that the plant is an *N*th plant and located in the US. In order to identify the most economic process configuration, two approaches were utilized. They are net present value (NPV) and minimum product selling price (MPSP). NPVs were applied for comparing the economy of Scenarios (1-5) and studying the sensitivity of economic feasibility with respect to hydrogen price. MPSPs were applied for comparison with naphtha-derived products. The NPVs of all the scenarios were evaluated based on the data from process simulator. For the case of conventional process equipment (such as distillation, vessels, compressors, cyclone, etc.), the purchased and installed equipment costs were calculated using Aspen Economic Analyzer™. However costing of nonconventional equipment (*e.g.*, reformer) was conducted by scaling up/down according to the following relation and with reference to the economic data from literature [37]:

$$New\ cost = Base\ cost * \left(\frac{New\ size}{Base\ size}\right)^{f_{scale}} \quad (1)$$

Once the total purchased equipment costs (TPEC) are estimated, the total indirect costs (TIC) are calculated including engineering (32% of TPEC), construction (34% of TPEC), legal and contractors fees (23% of TPEC) and project contingency (37% of TPEC). The fixed capital investment (FCI) is the sum of Total Direct Installed Costs (TDC) and TIC. The total capital costs include FCI and land cost (6% of TPEC) and the working capital (5% FCI) (Jones *et al*. 2009). The variable operating costs including raw materials, utilities, and waste disposal charges are summarized in Table 4. The fixed operating costs including labor, overheads (95% of labor cost), maintenance (4% of TCI), and insurance (4% of TCI) are scaled up based on Philipp, *et al*.'s study [46].

Table 4. Summary of variable operating cost

Materials/Chemicals/Utilities	Cost	Reference
Hybrid poplar	50.07 [$/short ton]	[36]
Natural gas	3.89 [$/1000scf]	[47]
Catalyst (Ru/C)	5.6 [$/kg]	[39]
Catalyst (Pt/C)	56.29 [$/kg]	[39]
Catalyst (Zeolite)	1.6 [$/kg]	[39]
Fresh water	0.05 [$/1000 gallon]	[49]
Electricity	37.02 [$/MWh]	[48]
Disposal of ash	18 [$/short ton]	[36]
Steam	4.3×10^{-3} - 4.5×10^{-3} [$/kg][a]	[49]
Refrigerant	1.08×10^{-5} – 4.51×10^{-5} [$/kg][b]	[49]
Cooling water	4.43×10^{-6} $/kg	[49]

Note: [a] varied for steam with different pressures; [b] varied for different types of refrigerants.

This paper should be cited at:
Sharifzadeh M*, Wang L., Shah N., (2015). Decarbonisation of olefin processes using biomass pyrolysis oil. *Applied Energy*, 149, 404–414, (Link).

2.4.2. Discounted cash flow method

The NPVs were calculated using a discounted cash flow method (10% discount rate) for a period of 20 years, which is the assumed plant lifetime. The plant was assumed to be 100% equity [46] with 2.5 years as a construction period and 6 months as the start-up time [36]. Prices of the products are summarized in Table 5. All costs in this study were indexed to the reference year of 2012 and the NPV of the project is reported as 2012 USD. The MPSPs is calculated using a discounted cash flow analysis and refers the product price at which the net present value of the project is zero at a set discounted rate of 10%. Since the process produces an array of olefins and aromatics, the MPSP for each product was estimated regarding to their ratio to the reference product (Ethylene in our study). These ratios were calculated based on their market prices (Table 5).

Table 5. Summary of the price of the petroleum-derived products

Bio-based chemicals	Price [$/kg]	Reference
Ethane	0.45	[50]
Benzene	0.85	[39]
Toluene	0.71	[39]
Butylene	0.75	[39]
Ethylene	1.49	[39]
Propylene	1.58	[39]
Propane	1.55	[51]
Butane	0.88	[51]
Indene+ Naphthalene,	0.85	[39]
Ethyl benzene+ Styrene+ Xylene	1.12 (average)	[39]
WIBO	0.02	[39]

2.5. Life Cycle Analysis for GHG emissions calculation

Life Cycle Analysis (LCA) approach was applied to calculate the GHG emissions for bio-based products through their 'Cradle-to-Grave' life cycles. The function unit is defined as '1 kg bio-based chemical product'. The whole life cycle includes feedstock cultivation (hybrid poplar), production of bio-based chemicals in biorefinery, transportation (raw materials, intermediate products, and final products), and end use of bio-based chemicals. The inventory data for hybrid poplar cultivation are adopted from Gasol *et al*.'s study [52] and the mass balance including chemical utilization and energy demand in bio-based chemicals production process are obtained from ASPEN Plus process simulations. The GHG emission factors for inputs in hybrid poplar cultivation, bio-based chemicals production, and transportation are taken from the Ecoinvent database V2.2 [53]. In bio-based chemicals production process, CO_2 is emitted from pyrolysis, reaction and separation sections. The GHG emissions resulted in waste treatment, *e.g.* solid residual disposal and wastewater treatment are also considered and they are estimated based on the inventory data from Ecoinvent database V2.2 [53]. The organic carbon sequestered in biomass and the life cycle impacts of the production

processes are allocated to products based on the mass basis. For simplicity, all carbon in bio-based chemicals is assumed to be released as carbon dioxide completely in their end use. The impacts of machinery, infrastructure and land use change are not included in our system boundary.

3. Results and discussions

3.1. Carbon conversion efficiency

Fig. 4 shows the results for the carbon yield distributions. They suggest that Scenarios (2) and (5) are the most promising configurations from the carbon yield point of view. While Scenario (5) produces products of higher quality (less coke, COx and heavy ends), the quantity of the products is larger in Scenario (2) because it processes the whole crude bio-oil (WIBO and WSBO). As discussed in the flexibility optimization, Scenario (5) is more preferable for producing olefins. However, Scenario (2) produces more aromatics. Scenario (1) is the least efficient scenario as zeolite cracking, in the absence of hydrodeoxygenation, converts half of the bio-oil to coke. Scenario (3) has the lowest conversion efficiencies as it only processes WSBO and produces low quality products.

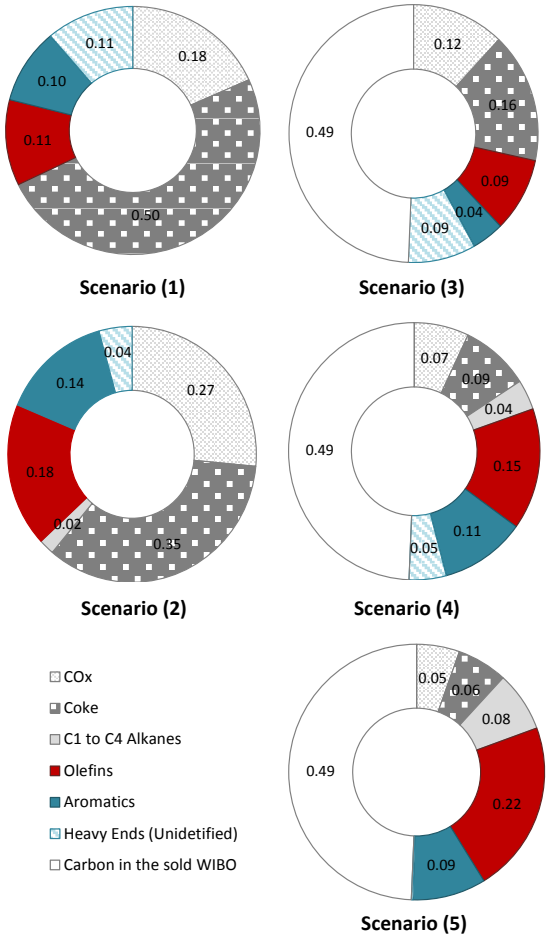

Fig. 4. The carbon yield distributions for scenarios 1-5 for different products

This paper should be cited at:
Sharifzadeh M*, Wang L., Shah N., (2015). Decarbonisation of olefin processes using biomass pyrolysis oil. *Applied Energy*, 149, 404–414, (Link).

3.2. Economic assessment

Table 6 reports the net present values (NPVs) of the five scenarios. Since the process economy was found very sensitive to the price of hydrogen, a sensitivity analysis was performed for different hydrogen prices in the range of 1.5-12 ($/kg) [7]. Table 6 shows that for a lower hydrogen price (1.5 $/kg), Scenario (5) is the most profitable configuration. However, as the price of hydrogen increases (2.5-5 $/kg), Scenario (2) becomes more attractive. The aforementioned results can also be presented in terms of internal rate of return (IRR) of each scenario, which is the rate of return that makes NPV equal to zero. Here, the calculated IRR values for the fifth scenario depend on the price of hydrogen and are 16.5%,12.6%, 9% at hydrogen prices of 1.5 $/kg and 2.5 $/kg and 3.3 $/kg, respectively. Similar IRR values for the second scenario are 15.2% 14.4%, 13.7%, respectively. These values are comparable with the studied scenarios by Zhang et al. [40], (7.6-13.3%). The differences are due to various assumptions on biomass cost, fixed capital cost and economic assessment parameters etc. It is notable that only for high hydrogen prices (>5 $/kg), reforming the water insoluble bio-oil (WIBO) would be attractive, which should be attributed to the low hydrogen content of WIBO [54]. The IRR value for the fifth scenario with a reformer is 11.8%.

Fig. 5 shows the results of break-down of the required capital investment for different section. The highest investment is needed for the pyrolysis section which processes a large amount of biomass. The value is similar for all scenarios. The capital requirement for the upgrading section depends on the number of reactors and the volume of the processed bio-oil. In that regard, Scenarios 2 and 5 are the most costly sections. The largest costs of the separation section belong to Scenario 2, due to a larger amount of reaction effluents (including CO_2). The highest required capital investment belongs to Scenario 5 w/ reformer due to the additional processing step. Fig. 6 shows the breakdown of operating costs. The biomass feedstock is similar in all the scenarios. However, the costs of other feedstocks (Hydrogen/water/caustic) are highest for Scenario 2. Scenario 5 with the reformer requires the highest electricity costs for operating the air compressor, reformer fans, and air-coolers.

Table 6. Net present value (NPV) for different process configurations as a function of hydrogen price.

H2	NPV MM$					
Price ($/kg)	**SC1**	**SC2**	**SC3**	**SC4**	**SC5**	**SC5 w/ reformer**
1.5	-101.97	**60.13**	-183.05	-9.36	**77.50**	**14.34**
2.5	-102.22	**47.81**	-183.28	-45.67	**22.47**	**14.34**
5	-102.85	**17.02**	-183.84	-160.27	-125.59	**14.34**
7.5	-103.47	-13.78	-184.39	-298.01	-333.07	**14.34**
12	-104.60	-69.20	-185.40	-549.44	-713.63	**14.34**

This paper should be cited at:
Sharifzadeh M*, Wang L., Shah N., (2015). Decarbonisation of olefin processes using biomass pyrolysis oil. *Applied Energy*, 149, 404–414, (Link).

381 **Table 7. Minimum product Selling Price (MPSP) for different scenarios. These grey cells are more economic**
382 **compared to the naphtha-based products in Table 5.**
383 **GHG emissions**

Product	SC1	SC2	SC3	SC4	SC5	SC5 w/ reformer
Ethane	0.58	**0.40**	0.71	0.46	**0.39**	**0.44**
Benzene	1.10	**0.76**	1.34	0.87	**0.75**	**0.83**
Toluene	0.92	**0.63**	1.12	0.72	**0.62**	**0.69**
Butylene	0.97	**0.67**	1.18	0.76	**0.66**	**0.73**
Ethylene	1.93	**1.33**	2.35	1.52	**1.31**	**1.46**
Propylene	2.05	**1.41**	2.49	1.61	**1.39**	**1.54**
Propane	2.01	**1.38**	2.45	1.58	**1.36**	**1.51**
Butane	1.14	**0.78**	1.39	0.90	**0.77**	**0.86**
Ethyl Benzene Styrene Xylene	1.10	**0.76**	1.34	0.87	**0.75**	**0.83**
Indene+ Naphthalene	1.46	**1.00**	1.77	1.14	**0.99**	**1.10**
WIBO	0.00	**0.00**	0.03	0.02	**0.02**	**0.02**

384

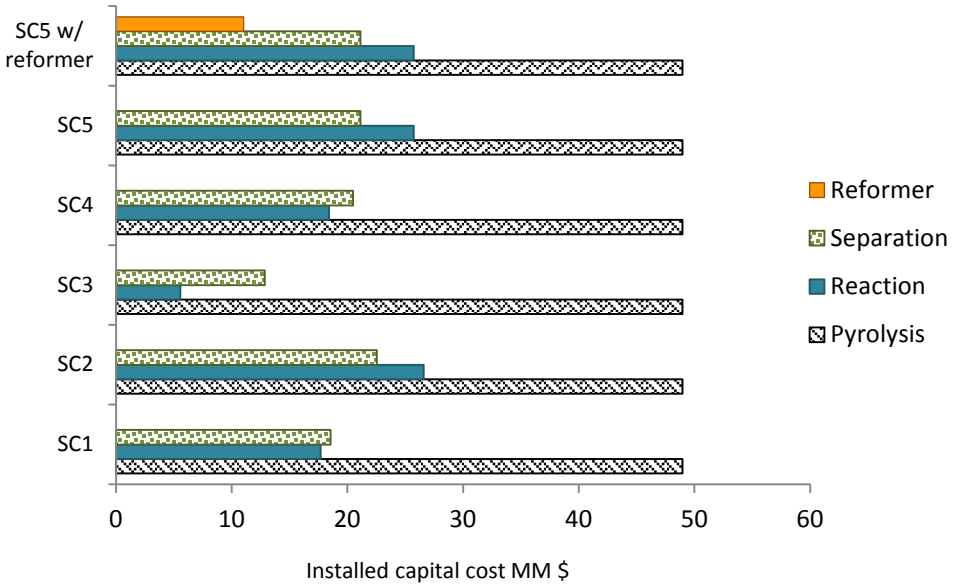

385
386 **Fig. 5. The required capital investment for different processing for different scenarios.**

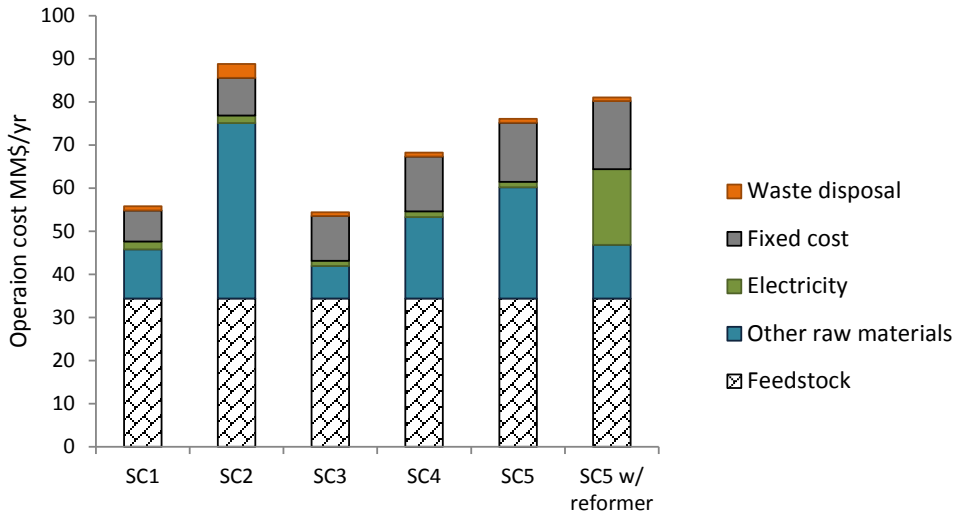

387
388 **Fig. 6. The operating costs for different scenarios.**

Table 7 reports the minimum product selling prices (MPSPs) for Scenarios (1-5) based on cheap hydrogen (1.5 $/kg) in addition to Scenario 5 w/ reformer, where WIBO is reformed for hydrogen production. These values are comparable with the prices of the petroleum-derived products in Table 5. The competitive scenarios are Scenario 2 and Scenario 5. For example, the price of ethylene when derived from petroleum is 1.49 $/kg, (Table 4). By comparison, the price of ethylene in Scenarios 2, 5 and 5 w/ reformer are 1.33 $/kg, 1.31 $/kg, 1.46 $/kg, respectively.

The Table 8 lists the 'Cradle-to-Grave' GHG emissions for each bio-based chemical product. It shows that the Scenarios 2 delivers the lowest GHG emission factors for most of available products. This is due to exploitation of the whole bio-oil (WSBO and WIBO) rather than a fraction of it. Scenario 1 requires no natural gas or hydrogen but a large amount of steam, leading to higher GHG emission factors than those in Scenario 2 which is energy self-efficient. In general Scenario 5s (with and without reformer) have higher GHG emission factors compared with other scenarios mainly due to their larger natural gas consumption for reforming WIBO.

Fig. 7 indicates the contribution results for GHG emissions of ethylene which is a main product in most of scenarios. The 'above-the-line' scores are environmental burdens while the 'below-the-line' ones are environmental credits. In our case, the 'below-the-line' scores are carbon sequestered in poplar biomass which is partially off-set by GHG emissions released in bio-based chemical production process and end use. Scenarios 1, 2 and 5 w/ reformer have the similar contributions whilst the other four share the similarity. This is because in Scenario 3-5 the total lifecycle impact is mainly allocated to WIBO due to its large amount of mass flow compared to other bio-based chemical products. Therefore the contribution of each process to the overall GHG emissions of ethylene is very small in Scenario 3-5. In Scenario 1, it is indicated that contributions by the poplar cultivation process (1.4% of the environmental burdens), catalyst production (0.05%), electricity (0.1%), transport (0.06%) and waste disposal (0.4%) are negligible. The main contributors apart from end use are emissions to air (22%) and steam production (7%) from burning coke. Overall, Scenario 5 with the reformer delivers the best economic feasibility and is independence of fluctuations in hydrogen price; however, it has the worst GHG emissions performance. If the hydrogen price remain lower than 5 $/kg, SC2 will become economically feasible (Table 6) and delivers the best GHG emissions performance among the five scenarios studied.

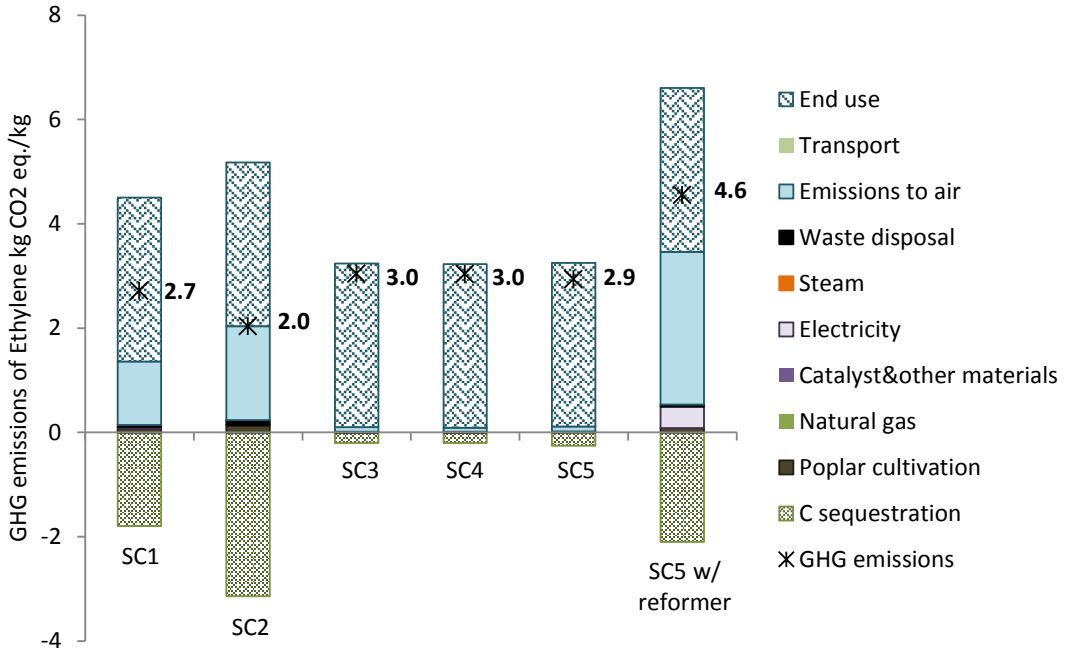

Fig. 7. Contribution analysis for GHG emissions of Ethylene in six scenarios (Functional Unit: 1kg, * indicates the GHG emission factors for Ethylene in each scenario)

Table 8 compares the GHG emissions of the six scenarios for the ethylene product with the GHG emissions of ethylene produced from naphtha, ethane, or biomass (wood, cassava, corn, and municipal solid waste). This table suggests that for example, ethylene production in the SC2 results in 44% X% lower GHG emissions, compared to the naphtha pathway, which should be attributed to the biogenic carbon sequestered in the biomass through photosynthesis process. In general, Table 9 suggests that the proposed pathway (pyrolysis followed by catalytic upgrading) features a better GHG footprint compared to other renewable pathways where biomass is firstly converted to ethanol, because their longer conversion processes involve enzyme usage as a large GHG emissions contributor.

Table 8. GHG emissions (kg CO_2 eq./kg) for each bio-based chemical product in six scenarios (Grey cells show the lowest GHG emissions for each bio-based chemical and bolded cell show the highest)

g CO_2 equivalent/kg product	SC1	SC2	SC3	SC4	SC5	SC5 w/ reformer
Ethane	0.00	2.90	0.00	2.94	2.90	**3.39**
Benzene	3.27	3.13	3.36	3.34	3.31	**3.86**
Toluene	3.07	2.77	3.30	3.24	3.22	**4.22**
Butylene	3.04	2.90	3.11	3.10	3.05	**3.77**
Ethylene	2.72	2.04	3.04	3.03	2.94	**4.55**
Propylene	2.84	2.38	3.03	2.96	2.80	**5.52**
Propane	0.00	2.97	0.00	3.00	2.97	**3.43**
Butane	0.00	2.97	0.00	3.01	2.98	**3.42**
E-benzene, Styrene, Xylene	3.12	2.63	3.30	3.32	3.27	**3.74**
Indene+ Naphthalene	3.33	3.39	3.41	3.33	3.35	**3.82**
WIBO	0.00	0.00	0.42	0.69	0.13	**0.00**

This paper should be cited at:
Sharifzadeh M*, Wang L., Shah N., (2015). Decarbonisation of olefin processes using biomass pyrolysis oil. *Applied Energy*, 149, 404–414, (Link).

Table 9. GHG emissions (kg CO_2 eq./kg) for the ethylene product in six scenarios in comparison with other petroleum-based and biomass-based pathways.

Feedstock	CO_2 eq. g/g	Technology	Ref
SC1	2.72	Pyrolysis / upgrading	
SC2	2.04	Pyrolysis / upgrading	
SC3	3.04	Pyrolysis / upgrading	
SC4	3.03	Pyrolysis / upgrading	
SC5	2.94	Pyrolysis / upgrading	
SC5 w/ reformer	4.55	Pyrolysis / upgrading	
Naphtha [(a)]	3.63	Hydrocracking	[1]
Ethane [(a)]	3.56	Hydrocracking	[1]
MSW[(b)]	4.9-12.6	Fischer-Tropsch Gasification	[2]
Ethanol (corn)	3.81	Enzymatic hydrolysis	[1]
Ethanol (corn)	3.4	Enzymatic hydrolysis	[3]
Ethanol (cassava)	5.6	Enzymatic hydrolysis	[3]
Ethanol (wood)[(c)]	0.9-5.6	Enzymatic hydrolysis	[4]

(a) The GHG emissions reported in Ghanta *et al.*'s study [1] are for 'cradle-to-gate' ethylene production excluding the end use phase. In the present study, the 'cradle-to-grave' value was calculated by adding GHG emissions released in its end use by assuming that all carbon in ethylene is turned to carbon dioxide. (b) MSW refers to municipal solid waste. The variations reflect the different gasification technologies (*i.e.* Battelle, MTCI, and Choren). (c) The highest value represents the current technology whilst the lowest boundary represents the prospective technology with higher enzyme activity and lower enzyme loading in enzymatic hydrolysis of ethanol production.

4. Conclusions

The current state of industry is that many energy-intensive processes are relatively mature and the number of new processes that are being built is significantly less than the number of operating processes. This observation suggests that an important pathway toward decarbonisation of industrial processes is to substitute their feedstock with biomass-derived feedstocks and retrofit them using green technologies. The present paper proposed retrofitting a conventional olefin process by substituting its feedstock (naphtha) with bio-oil. Here, the enabling technology is the integrated catalytic bio-oil upgrading reactors which produce a mixture very similar to naphtha-based cracked gas. In the present research, it was shown that by using this technology, it is possible to retrofit current olefin processes to flexibly produce key olefins and aromatics. Furthermore, due to aforementioned synergies, retrofitting current olefin processes requires minimal changes in the separation network. The present paper also studied various process configurations, in which the whole bio-oil or only a fraction of it (only the water soluble part) is processed. It was shown that the profitability of the process may strongly depend on the hydrogen prices. For example, importing hydrogen for the prices over 6 $/kg will results in bio-based chemicals which are generally more expensive than petroleum-derived products. It was proposed that for hydrogen prices higher than 6 $/kg, water insoluble bio-oil (WIBO) could be reformed to produce the required hydrogen. From a GHG emissions point of view, the results concluded that there was a remarkable improvement of up to 44% reductions in the carbon footprint of the olefin process in certain scenarios.

This paper should be cited at:
Sharifzadeh M*, Wang L., Shah N., (2015). Decarbonisation of olefin processes using biomass pyrolysis oil. *Applied Energy*, 149, 404–414, (Link).

The present research provided a proof of concept for decarbonisation of the olefin industries, based on lab-scale experimental data. We believe that the future research should be in the following directions:

- Developing kinetic correlations for detailed reactor design, scale up and optimization,
- Evaluating the possibility of co-feeding bio-oil and conventional feedstocks (*e.g.*, naphtha),
- Investigating the implication of retrofitting existing processes due to fouling and corrosion,
- Detailed design of control systems for the catalytic bio-oil upgrading reactors.

5. Acknowledgements

Dr Mahdi Sharifzadeh would like to thank the financial supports of the Carbon Trust (CT) and the Department of Energy & Climate Change (DECC), UK, for his postdoctoral studies.

6. References

1. Ghanta M, Fahey D, Subramaniam B. Environmental impacts of ethylene production from diverse feedstocks and energy sources. Appl Petrochem Res, 2014; 4 (2): 167-179.

2. Nuss P, Gardner KH, Bringezu S. Environmental Implications and Costs of Municipal Solid Waste-Derived Ethylene. J Ind Ecol, 2013; 17: 912–925.

3. Hong J, Zhang Y, Xu X, Li X. Life cycle assessment of corn- and cassava-based ethylene production. Biomass Bioenergy, 2014; 67: 304-311.

4. Liptow C, Tillman A, Janssen M, Wallberg O, Taylor GA. Ethylene based on woody biomass—what are environmental key issues of a possible future Swedish production on industrial scale. Int J Life Cycle Assess, 2013; 18: 1071–1081.

5. Xiang D, Qian Y, Man Y, Yang S. Techno-economic analysis of the coal-to-olefins process in comparison with the oil-to-olefins process. Appl Energy, 2014; 113: 639–647.

6. Demirbas MF. Biorefineries for biofuel upgrading: A critical review. Appl Energy, 2009; 86: S151–S161

7. Vispute TP, Zhang H, Sanna A, Xiao R, Huber GW. Renewable chemical commodity feedstocks from integrated catalytic processing of pyrolysis oils. Science, 2010; 330: 1222-1227.

8. Mettler MS, Vlachos DG, Dauenhauer PJ, Energy Environ. Sci., 2012; 5: 7797.

9. Azeez AM, Meier D, Odermatt J, Willner T. Fast Pyrolysis of African and European Lignocellulosic

487 Biomasses Using Py-GC/MS and Fluidized Bed Reactor. Energy Fuels, 2010; 24: 2078–2085.

488 10. Ben H, Ragauskas AJ. NMR Characterization of Pyrolysis Oils from Kraft Lignin. Energy Fuels,
489 2011; 25: 2322–2332.

490 11. Ben H, Ragauskas AJ. Comparison for the compositions of fast and slow pyrolysis oils by NMR
491 Characterization. Bioresour Technol, 2013; 147: 577–584.

492 12. White JE, Catallo WJ, Legendre BL. Biomass pyrolysis kinetics: A comparative critical review with
493 relevant agricultural residue case studies. J Anal Appl Pyrol, 2011; 91: 1–33.

494 13. Papadikis K, Gu S, Bridgwater AV, Gerhauser H. Application of CFD to model fast pyrolysis of
495 biomass. Fuel Process Technol, 2009; 90: 504–512.

496 14. Isahak WNRW, Hisham MWM, Yarmo MA, Hin TY. A review on bio-oil production from biomass
497 by using pyrolysis method. Renew. Sust. Energ. Rev., 2012; 16: 5910–5923.

498 15. Motasemi F, Afzal MT. A review on the microwave-assisted pyrolysis technique. Renew. Sust.
499 Energ. Rev., 2013, 28, 317–330.

500 16. Borges FC, Du Z, Xie Q, Trierweiler JO, Cheng Y, Wan Y, Liu Y, Zhu R, Lin X, Chen P, Ruan R. Fast
501 microwave assisted pyrolysis of biomass using microwave Absorbent. Bioresour Technol, 2014;
502 156: 267–274.

503 17. Akhtar J, Amin NS. A review on operating parameters for optimum liquid oil yield in biomass
504 pyrolysis. Renew. Sust. Energ. Rev., 2012; 16: 5101–5109.

505 18. Zhang L, Liu R, Yin R, Mei Y. Upgrading of bio-oil from biomass fast pyrolysis in China: A review.
506 Renew Sust Energ Rev, 2013; 24: 66–72.

507 19. Sadhukhan J. Multiscale simulation for high efficiency biodiesel process intensification. Computer
508 Aided Chemical Engineering, 2012; 30: 1023-1027.

509 20. Brown TR, Thilakaratne R, Brown RC, Hu G. Techno-economic analysis of biomass to
510 transportation fuels and electricity via fast pyrolysis and hydroprocessing. Fuel, 2013; 106: 463–
511 469.

512 21. Zhu Y, Biddy MJ, Jones SB, Elliott DC, Schmidt AJ. Techno-economic analysis of liquid fuel
513 production from woody biomass via hydrothermal liquefaction (HTL) and upgrading. Appl Energy,
514 2014; 129: 384–394.

515 22. Gebreslassie BH, Slivinsky M, Wang B, You F. Life cycle optimization for sustainable design and
516 operations of hydrocarbon biorefinery via fast pyrolysis, hydrotreating and hydrocracking.

517 Comput Chem Eng, 2013; 50: 71– 91.

518 23. Kim J, Realff MJ, Lee JH, Whittaker C, Furtner L. Design of biomass processing network for biofuel
519 production using an MILP model. Biomass Bioenerg, 2011; 35: 853-871.

520 24. Akgul O, Shah N, Papageorgiou LG. Economic optimisation of a UK advanced biofuel supply chain
521 Economic optimisation of a UK advanced biofuel supply chain. Biomass Bioenerg, 2012; 41: 57–
522 72.

523 25. Braimakisa K, Atsoniosa K, Panopoulos KD, Karellas S, Kakaras E, Economic evaluation of
524 decentralized pyrolysis for the production of bio-oil as an energy carrier for improved logistics
525 towards a large centralized gasification plant. Renew. Sust. Energ. Rev., 2014; 35: 57–72.

526 26. Meier D, Beld B, Bridgwater AV, Elliott DC, Oasmaa A, Preto F. State-of-the-art of fast pyrolysis in
527 IEA bioenergy member countries. Renew Sust Energ Rev, 2013; 20: 619–641.

528 27. Saidi M, Samimi F, Karimipourfard D, Nimmanwudipong T, Gates BC, Rahimpour MR. Upgrading
529 of lignin-derived bio-oils by catalytic hydrodeoxygenation. Energy Environ. Sci., 2014, 7, 103–129.
530 Energy Environ. Sci., 2011, 4, 985.

531 28. Baker EG, Elliott DC. Catalytic upgrading of biomass pyrolysis oils, Elsevier Appl Sci Publ Ltd,
532 Barking Essex, 1988, pp. 883–895.

533 29. Demirbas A. Competitive liquid biofuels from biomass. Appl Energy, 2011; 88: 17–28

534 30. Ibáñez M, Valle B, Bilbao J, Gayubo AG, Castaño P, Effect of operating conditions on the coke
535 nature and HZSM-5 catalysts deactivation in the transformation of crude bio-oil into
536 hydrocarbons. Catalysis Today, 2012; 195 (1): 106–113.

537 31. Xiu S, Shahbazi A. Bio-oil production and upgrading research: A review. Renew. Sust. Energ. Rev.,
538 2012; 16: 4406–4414.

539 32. Taarning E, Osmundsen CM, Yang X, Voss B, Andersen SI, Christensen CH. Zeolite-catalyzed
540 biomass conversion to fuels and chemicals. Energy Environ. Sci., 2011; 4: 793–804.

541 33. Ragauskas J, Williams CK, Davison BH, Britovsek G, Cairney J, Eckert CA, Frederick Jr WJ, Hallett
542 JP, Leak DJ, Liotta CL, Mielenz JR, Murphy R, Templer R, Tschaplinski T. The Path Forward for
543 Biofuels and Biomaterials. Science, 2006; 311: 484-489.

544 34. Peterson AA, Vogel F, Lachance RP, Froling M, Antal Jr. MJ, Tester JW. Thermochemical biofuel
545 production in hydrothermal media: A review of sub- and supercritical water technologies. Energy
546 Environ. Sci., 2008; 1: 32–65.

This paper should be cited at:
Sharifzadeh M*, Wang L., Shah N., (2015). Decarbonisation of olefin processes using biomass pyrolysis oil. *Applied Energy*, 149, 404–414, (Link).

547 35. Ruiz JCS, Dumesic JA. Catalytic routes for the conversion of biomass into liquid hydrocarbon
548 transportation fuels. Energy Environ. Sci., 2011, 4, 83.

549 36. Jones SB, Holladay JE, Valkenburg C, Stevens DJ, Walton CW, Kinchin C, Elliott DC, Czernik S.
550 Production of Gasoline and Diesel from Biomass via Fast Pyrolysis, Hydrotreating and
551 Hydrocracking: A Design Case, U.S. Department of Energy. 2009, Technical Report.

552 37. Wright MM, Daugaard DE, Satrio JA, Brown RC, Techno-economic analysis of biomass fast
553 pyrolysis to transportation fuels. Fuel, 2010; 89 (1): S2-S10.

554 38. Shemfe MB, Panneerselvam Ranganathan SG, Techno-economic performance analysis of biofuel
555 production and miniature electric power generation from biomass fast pyrolysis and bio-oil
556 upgrading, Fuel, 2015; 143: 361-372.

557 39. Brown TR, Zhang Y, Hu G, Brown RC. Techno-economic analysis of biobased chemicals
558 production via integrated catalytic processing. Biofuels, Bioprod. Bioref. 2012; 6: 73–87.

559 40. Zhang Y, Brown TR, Hu G, Brown RC, Techno-economic analysis of two bio-oil upgrading
560 pathways, *Chemical Engineering Journal*, 2013; 225: 895-904.

561 41. Jenkins BM, Baxter LL, Miles Jr. TR, Miles TR. Combustion properties of biomass. Fuel processing
562 technology, 1998; 54: 17–46.

563 42. Sharifzadeh M, Rashtchian D, Pishvaie MR, Thornhill NF. Energy induced separation network
564 synthesis of an olefin compression section: a case study. Ind Eng Chem Res, 50; 3: 1610-1623.

565 43. Othmers K. Encyclopedia of Chemical Technology, 4th ed.; Wiley: New York, 1998.

566 44. Sipila K, Kuoppala E, Fagernas L, Oasmaa A, Characterization of biomass-based Flash pyrolysis
567 oils, Biomass Bioenergy, 1998; 14: 103-113.

568 45. Vispute TP and Huber GW. Production of hydrogen, alkanes and polyols by aqueous phase
569 processing of wood-derived pyrolysis oils. Green Chem., 2009; 11: 1433–1445.

570 46. Phillips S, Aden A, Jechura J, Dayton D, T Eggeman. 2007, National Renewable Energy Laboratory
571 (NREL), Thermochemical Ethanol via Indirect Gasification and Mixed Alcohol Synthesis of
572 Lignocellulosic Biomass, Technical Report, NREL/TP-510-41168.

573 47. US Energy Information Administration, Natural Gas
574 Prices, URL:http://www.eia.gov/dnav/ng/ng_pri_sum_dcu_nus_a.htm , accessed August 2014

575 48. US Energy Information Administration, Electricity Wholesale Market, Data,
576 URL: http://www.eia.gov/electricity/wholesale/ , accessed August 2014.

This paper should be cited at:
Sharifzadeh M*, Wang L., Shah N., (2015). Decarbonisation of olefin processes using biomass pyrolysis oil. *Applied Energy*, 149, 404–414, (Link).

577 49. Davis R, Aden A, Pienkos PT. Techno-economic analysis of autotrophic microalgae for fuel
578 production. Appl Energy, 2011; 88: 3524–3531.

579 49. Aspen Plus software tool, V8.4. Apsen Tech.

580 50. Ethane spot price. URL:http://www.platts.com/news-feature/2013/petrochemicals/global-
581 margins/us_natgas , accessed August 2014.

582 51. US Energy Information Administration, Natural gas liquids prices,
583 2013b, URL:http://www.eia.gov/todayinenergy/detail.cfm?id=12291, accessed August 2014.

584 52. Gasol CM, Gabarrell X, Anton A, Rigola M, Carrasco J, Ciriae P, Rieradevall J. LCA of poplar
585 bioenergy system compared with Brassica carinata energy crop and natural gas in regional
586 scenario. Biomass Bioenerg, 2009; 33: 119–129.

587 53. Jungbluth N, Faist Emmenegger M, Dinkel F, Stettler C, Doka G, Chudacoff M, Dauriat A,
588 Gnansounou E, Sutter J, Spielmann M, Kljun N, Keller M, Schleiss K. Life cycle inventories of
589 Bioenergy. 2007, Swiss Centre for Life Cycle Inventories, Dübendorf.

590 54. Marker, TL 2005, Opportunities for biorenewables in oil refineries. Final Technical Report. United
591 States. DOEGO15085, UOP, Des Plaines, IL.

This paper should be cited at:
Sharifzadeh M*, Wang L., Shah N., (2015). Decarbonisation of olefin processes using biomass pyrolysis oil. *Applied Energy*, 149, 404–414, (Link).

Decarbonisation of Olefin Processes using Biomass Pyrolysis Oil

Sharifzadeh M [a]*[1], Wang L[b] and Shah N[a]
[a] Centre for Process Systems Engineering (CPSE), Department of Chemical Engineering, Imperial College London.
[b] Centre for Environmental Policy, Imperial College London.

Electronic Supplementary Materials

The present document is prepared to complement the manuscript and provide additional information. The features of interest include the process description and the flow diagrams of the sub-processes (Sections 100-700 in Figs. 1a and 1b of the manuscript), the required retrofit for adaptation to bio-oil feedstock and the assumptions used for modelling each section.

Section 100: Biomass pyrolysis

The pyrolysis section is shown in Fig. S1, adapted from Jones, *et al*., [S1]. The feedstock of this section is wood (hybrid poplar) and the product is the pyrolysis oil, also known as bio-oil. This section consists of a high temperature short residence time fluidized bed reactor, where biomass is converted to a mixture of light gases, condensable gases, water and char. The produced char is separated in a gas cyclone and burned in a furnace in order to supply energy for the endothermic reactions. A part of exhaust gas is also used to provide the required heat to the reactor. The remaining exhausts are exploited in the biomass drier. The rest of the reaction effluents are quenched rapidly in order to suppress degrading reactions. Light gases are recycled to the reactor/combustor and the condensates called bio-oil is sent for upgrading to Section 200. The produced ash is landfilled and the associated costs were includes in the economic analysis. All the modelling assumptions in this section are based on [S1]. The carbon balance around Section 100 is shown in Table S2, and explained later.

Section 200: multi stage catalytic upgrading reaction network

The condensable effluents of biomass pyrolysis, also known as bio-oil, form a brownish mixture, which cannot be immediately used as a transportation fuel or biochemical. Therefore, the aim of Section 200 is to upgrade the bio-oil in a sequence of catalytic reactors, proposed by Vispute, *et al.* [S2]. In this section, firstly, the crude bio-oil is mixed with water at a mass ratio of 1:4. Then, the mixture is separated into two liquid phases. The aqueous phase, also called water soluble bio-oil (WSBO), is sent to a low-temperature hydro-processing unit which operates at 398 K and 100 bar. This is the highest temperature with no risk of catalyst coking and reactor plugging. Supported Ru was identified as the most active and selective catalyst for aqueous phase hydro-processing. The partially stabilized bio-oil is then fed to the second hydrogenation stage that operates at 523 K and 100 bar. Supported Pt was identified as the best catalyst for this stage with desirable properties such as high C-O hydrogenation and low C-C bond cleavage activities. The third reactor is a fluidized bed reactor that provides an upgrading step over the zeolite catalyst in order to produce olefins and aromatics. Vispute, *et al*.[S2] demonstrated that the yields of the aromatic and olefin products depends on the added hydrogen in the first two stages. Five process configurations were studied. They were:

- Scenario (1), where the crude bio-oil was directly sent to the zeolite upgrading stage;
- Scenario (2), where the crude bio-oil was firstly hydrotreated at the low temperature reactor and then processed in the zeolite upgrading reactor;
- Scenario (3), where water soluble bio-oil (WSBO) was directly sent to the zeolite upgrading stage;
- Scenario (4), where water soluble bio-oil (WSBO) was firstly hydrotreated at the low temperature reactor and then processed in the zeolite upgrading reactor;
- Scenario (5), where water soluble bio-oil (WSBO) was processed in all the three reactors.

An important advantage of multi-stage hydrogenation is to eliminate the risk of coke formation and catalyst deactivation.

[1] Corresponding author, E-mail: mahdi@imperial.ac.uk; Tel:+44(0)7517853422.

This paper should be cited at:
Sharifzadeh M*, Wang L., Shah N., (2015). Decarbonisation of olefin processes using biomass pyrolysis oil. *Applied Energy*, 149, 404–414, (Link).

Table S1 shows the flowrate and composition of the product stream leaving Section 200, for the aforementioned scenarios. The compositions adapted were from the results by Vispute, *et al*. [S2]. This table suggests that the upgraded pyrolysis oil is a complex mixture of unreacted hydrogen, C_1-C_4 alkanes, C_2-C_4 olefins, C_6-C_8 aromatics and heavy hydrocarbon. Therefore, the separation network requires a wide range of technologies and a high degree of energy recovery and heat integration, as discussed in the following.

Table S1. The composition (mass fraction) and flowrates of the product streams, used for modelling zeolite cracking reactor (R-203 in Fig S2) in different scenarios [S2]

	Scenario (1)	Scenario (2)	Scenario (3)	Scenario (4)	Scenario (5)
Feed	WIBO+ WSBO	WIBO+ WSBO	WSBO	WSBO	WSBO
Required hydrogen	None	0.9	None	4.8	8.1
Cox					
CO	0.2201	0.3479	0.2645	0.1197	0.1010
CO_2	0.1229	0.1029	0.1346	0.1652	0.1341
Coke	0.3460	0.2314	0.2046	0.1207	0.0941
C1 to C4 Alkanes					
Methane		0.0045		0.0174	0.0374
Ethane		0.0042		0.0163	0.0351
Propane		0.0041		0.0159	0.0343
n-Butane		0.0040		0.0157	0.0339
Olefins					
ETHYLENE	0.0474	0.0749	0.0569	0.0778	0.1200
Propylene	0.0335	0.0510	0.0628	0.1355	0.2018
Butylene	0.0106	0.0162	0.0171	0.0313	0.0533
Aromatics					
Benzene	0.0128	0.0176	0.0151	0.0286	0.0400
Toluene	0.0306	0.0393	0.0265	0.0747	0.0738
Xylenes	0.0178	0.0409	0.0119	0.0518	0.0288
Ethylbenzene	0.0015	0.0036	0.0007	0.0043	0.0035
Styrene	0.0030	0.0028	0.0014	0.0028	0.0019
Indene	0.0060	0.0000	0.0007	0.0021	0.0007
Naphthalene	0.0030	0.0014	0.0007	0.0000	0.0007
Unidentified	0.1447	0.0532	0.2026	0.1205	0.0055
Total flow [kg/h]	**39648**	**41434**	**22165**	**20251**	**18801**

Section 300: Primary fractionation/ water separation

Fig. S2 also shows the process flow diagram for Section 300. The product mixture includes heavy hydrocarbons such as Indene and Naphthalene which are denser than water and are separated in the primary distillation column. Due to large spectrum of hydrocarbons, sharp separation of Indene and Naphthalene in a single column is not economic and these products are therefore separated in a side stripper with the aid of high temperature steam. In addition, because of the high volume of the water employed by the hydrothermal reactions, it is necessary to separate and recycle water as soon as possible in order to avoid associated energy penalties. Therefore, water is separated in the water-wash tower and stripped in the sour water tower as shown in the Fig. 2S.

Section 400: Energy induced separation network (EISEN)

The remaining upgraded gaseous effluents are sent to an energy induced separation network (EISEN). This is a separation network in which both heat exchange and pressure adjustment are employed to separate olefins from aromatics. The EISEN is shown in Fig. 3S and consists of a multi-stage compression network, a caustic wash tower and a stripper. In each compression stage, the upgraded gas is compressed and then cooled in an interstage cooler using cooling water. The sequential compression and cooling result in condensation of water and aromatics. These condensates are sent to a stripper where the dissolved light gases are separated and

recycled. The bottom stream of the stripper contains the aromatic products. An absorber is designed between the fourth and fifth compressor stages, where the carbon oxides are separated from the mixture, using caustic. The condensates and gases of the fifth compression stage are sent to the cryogenic distillation train after drying.

Section 500: Cryogenic distillation of olefin products

The compressed streams from Section 400 are complex mixtures of alkanes and olefins, with very low boiling temperatures. Heat integration with product streams in addition to ethylene and propylene refrigerants are employed in order to liquefy the gaseous stream at around -87^{o}C and 36 bar. The compressed and refrigerated hydrocarbons are fed to a series of cryogenic distillation columns. Conventionally, in the first distillation column, *i.e.*, demethanizer, the unreacted hydrogen and methane are separated as the overhead product. Then, this stream is sent to a pressure swing adsorption (PSA) unit after exchanging heat with the compressed gases in the cold box. However, since no excess hydrogen was observed by Vispute, *et al*.,[S2] the PSA unit can be potentially excluded from the retrofitted process. The methane will be burnt as a fuel gas. The bottom product of the demethanizer is sent to deethanizer column where a mixture of ethylene and ethane are separated and sent to the C_2-splitter column. The pure ethylene product is separated in the C_2-splitter overhead and sent to storage. The bottom ethane product will be exploited as fuel gas after throttling and heat integration. The bottom stream of the deethanizer is sent to depropanizer and similarly the C_3 components are separated and sent to the C_3-plitter where relatively pure propane and propylene are produced. The propylene is a main olefin product and the propane will be used as a Fuel gas. The debutanizer column separates the C_4-cut products and the remaining aromatic which will be sent to the pyrolysis gasoline hydrogenation section. N-butane and butylene are resolved in the C_4-splitter. The justification for the choices of the column pressures was based on the availability of the ethylene and propylene refrigerants for the cooling duties of the condensers.

Section 600: Pyrolysis oil hydrogenation / Distillation of aromatic

The bottom stream of the stripper (Section 400) has very similar properties to gasoline. However, it contains small amounts of dissolved highly reactive olefins and if stored untreated, will suffer from polymerization and wax formation. Therefore, a mild hydrogenation is needed to eliminate any remaining unsaturated bounds. The reactor is operated at 26 bar and 160^{o}C. Then, the unreacted hydrogen is separated in two series hot and cold separators from aromatic products, which are sent to a distillation train where they are resolved to C_6, C_7 and C_{8+} products. The flow diagram of Section 600 is shown in Fig. S5.

Section 700: Hydrogen production

The organic phase, also called water insoluble bio-oil (WIBO), mostly consists of lignin-derived phenolic oligomers. In Scenarios 1-5, WIBO is sold as a low quality fuel. However, the results of economic analysis showed that the profitability of the process strongly depends on the price of hydrogen. Therefore, an additional study (Scenario 5 with reformer) was considered in which WIBO was reformed to produce the required hydrogen. The process flow diagram is shown in Fig. S6. The water insoluble is mixed with water and sent to the reformer where syngas a mixture of carbon oxides, hydrogen, and water, is formed. The overall hydrogen yield is further improved in a low temperature reactor, before being sent to the pressure swing adsorption (PSA) for separation. The tail gas (CO, CO_2 and unseparated hydrogen) is recycled to the reformer and burned in the combustion zone. The excess heat is used for producing steam.

Process modelling and implementation considerations

The bio-oil used in the Vispute, *et al*.'s study [S2] was supplied by NREL [S3] and was produced from pyrolyzing mixed wood. Therefore, the process throughput was chosen to be 2000 ton per day (tpd) of mixed wood. However, since the composition of the mixed wood was unknown, it was difficult to collect the required LCA inventory data. Therefore, in the present research the equivalent amount of hybrid polar which gives similar carbon flow in the bio-oil was chosen as the basis for the process modelling and LCA analysis. The results of these calculations are shown in Table S2. This table suggests that 1889 tpd of hybrid polar will result in the same carbon flow in the produced bio-oil as 2000 tpd of mixed wood. The required data for modelling pyrolysis section based on hybrid polar was based on [S1]. The inventory data for the hybrid polar cultivation was from Gasol, *et al.*'s study [S4].

This paper should be cited at:
Sharifzadeh M*, Wang L., Shah N., (2015). Decarbonisation of olefin processes using biomass pyrolysis oil. *Applied Energy*, 149, 404–414, (Link).

As, also mentioned in the manuscript, the process modelling was conducted using Aspen Plus™ simulator. The pyrolysis and upgrading reactors were modelled based on the yield data from [S2] and [S1], respectively. High purity chemicals were produced (> 0.99 mass fraction). ENRTL-RK method described the thermodynamic properties. The simulation of pyrolysis section was validated using the data from [S1]. The model of cryogenic section was validated using the data from Sharifzadeh, *et al*.'s study [S5]. The distillation columns were modelled using RADFRAC unit operation in Aspen Plus. The pressure swing adsorption was modelled using "SEP" unit operation in Aspen Plus, assuming 90% separation efficiency. Table S3 reports the modelling approach and operating conditions applied for simulating the main reactors. The pyrolysis reactor was modelled using the yield data from a previous study by DOE [S1]. The compositions and flowrates of the pyrolysis reactor feed and products are shown in Table S4. The integrated catalytic reactors were modelled using the experimental yield data from Vispute *et al*.'s study [S2], and [S5]. The elemental analysis used for modelling water soluble bio-oil (WSBO) and water insoluble bio-oil (WIBO) were from [S5] and are shown in Table S5. The product compositions of the low temperature hydrogenation reactor (R-201 in Fig S2) and the high temperature hydrogenation reactor (R-202 in Fig S2) are shown in Table S5. Table S1 showed the product compositions and flowrates of the zeolite cracking reactor (R-203 in Fig S2) in different scenarios (1-5), adapted from [S2]. Please note that the experimental results from [S2] were reported in terms of identified carbon contents. These results were converted to mass and mole fractions using molecular weight and molecular formula of each component. Table S1 also reported the amount of required hydrogen in each Scenario (1-5), [S2]. The pyrolysis gasoline hydrogenation reactor was modelled based on 100% conversion of olefins. The required amount of hydrogen was calculated based on the amount unsaturated carbon in the reactor feed. The reformer (R-601 in Figure S5) was modelled based on chemical equilibrium using Gibbs Free Energy minimization [S6]. The high temperature gas shift reactor was modelled based on 80% of conversion of CO though water-gas shift reaction [S1]. The costs of conventional unit operations (*e.g.*, distillations, compressors) were evaluated using Aspen Economic Analyzer™. The costs of nonconventional unit operations (*e.g.*, reformer, pyrolyzer) were calculated by scaling with respect to economic data from literature [S1].

References

[S1] Jones SB, Holladay JE, Valkenburg C, Stevens DJ, Walton CW, Kinchin C, Elliott DC, Czernik S. Production of Gasoline and Diesel from Biomass via Fast Pyrolysis, Hydrotreating and Hydrocracking: A Design Case, U.S. Department of Energy. 2009, Technical Report.

[S2] Vispute TP, Zhang H, Sanna A, Xiao R, Huber GW. Renewable chemical commodity feedstocks from integrated catalytic processing of pyrolysis oils. Science, 2010; 330: 1222-1227.

[S3] Brown TR, Zhang Y, Hu G, Brown RC. Techno-economic analysis of biobased chemicals production via integrated catalytic processing. Biofuels, Bioprod. Bioref. 2012; 6: 73–87.

[S4] Gasol CM, Gabarrell X, Anton A, Rigola M, Carrasco J, Ciriae P, Rieradevall J. LCA of poplar bioenergy system compared with Brassica carinata energy crop and natural gas in regional scenario. Biomass Bioenerg, 2009; 33: 119–129.

[S5] Vispute TP and Huber GW. Production of hydrogen, alkanes and polyols by aqueous phase processing of wood-derived pyrolysis oils. Green Chem., 2009; 11: 1433–1445.

[S6] Zhang Y, Brown TR, Hu G, Brown RC. Comparative techno-economic analysis of biohydrogen production via bio-oil gasification and bio-oil reforming. 2013; 51: 99–108.

This paper should be cited at:
Sharifzadeh M*, Wang L., Shah N., (2015). Decarbonisation of olefin processes using biomass pyrolysis oil. *Applied Energy*, 149, 404–414, (Link).

Table S2. The carbon balance around pyrolysis section for different feedstock: hybrid polar (present study) and mixed wood [S2]

	Hybrid poplar (present study)	Mixed Wood [S2]
Biomass (ton per day)	1889.441	2000
Carbon content in biomass (wt)	0.5029 [S1]	0.4751 [S3]
Carbon flow in biomass (Kg/h)	39591.7	39591.7
Pyrolysis carbon efficiency (wt%)*	70% [S2]	70% [S2]
Bio-oil (Kg/h)	61712.8	48835.5
Carbon content of bio-oil (wt)	0.449	0.5675
Carbon flow in the bio-oil (Kg/h)	27714.2	27714.2

*The pyrolysis carbon efficiency is defined as kg of carbon in bio-oil/ kg of carbon in biomass

Table S3. The modelling approach and operating conditions for major reactors.

Reactor	Description	T (K)	P (bara)	Modelling approach	Ref.
R101 (Fig S1)	Pyrolysis reactor	773	1.1	Yield	[S1]
R201 (Fig S2)	Low temperature hydrogenation reactor	398	100	Yield	[S2]
R202 (Fig S2)	High temperature hydrogenation reactor	523	100	Yield	[S2]
R203 (Fig S2)	Zeolite cracking reactor	873	1.01	Yield	[S2]
R601 (Fig S5)	Pyrolysis gasoline hydrogenation reactor	433	27	Conversion (100% olefins)	-
R701 (Fig S6)	Reformer reactor	1123	25.8	Chemical Equilibrium	[S1]
R-702 (Fig S6)	High temperature gas shift reactor	626	24.8	Conversion (80% CO)	[S1]

This paper should be cited at:
Sharifzadeh M*, Wang L., Shah N., (2015). Decarbonisation of olefin processes using biomass pyrolysis oil. *Applied Energy*, 149, 404–414, (Link).

Table S4. The mass fraction and flowrates of the feed and product streams of the pyrolysis reactor (R-101 in Fig S1). [S2]

	Feed	Fluidizing gas	Sand recycle	Products
	Mass fraction	Mass fraction	Mass fraction	Mass fraction
Oxygen	0.00000	0.00000	0.00000	0.00124
Nitrogen	0.00000	0.05216	0.00000	0.00340
Water	0.07000	0.00044	0.00000	0.01030
Hybrid Poplar	0.93000	0.00000	0.00000	0.00000
Hydrogen	0.00000	0.00215	0.00000	0.00045
Carbon	0.00000	0.00000	0.00000	0.00480
Carbon Monoxide	0.00000	0.85734	0.00000	0.05595
Carbon Dioxide	0.00000	0.04753	0.00000	0.00311
Methane	0.00000	0.00428	0.00000	0.00028
Ethylene	0.00000	0.01703	0.00000	0.00111
Propylene	0.00000	0.01768	0.00000	0.00116
Ammonia	0.00000	0.00138	0.00000	0.00009
Pyro-lignin	0.00000	0.00000	0.00000	0.02057
Cellobiose	0.00000	0.00000	0.00000	0.00724
Levoglucosan	0.00000	0.00000	0.00000	0.00190
Furfural	0.00000	0.00000	0.00000	0.00381
HydroxyAcetone	0.00000	0.00000	0.00000	0.00190
Acetic Acid	0.00000	0.00000	0.00000	0.00267
Ca	0.00000	0.00000	0.00000	0.00112
Sulphur	0.00000	0.00000	0.00000	0.00001
Calcium Chloride	0.00000	0.00000	0.00000	0.00002
Sand	0.00000	0.00000	1.00000	0.87888
Flowrate (lb/h)	197546	183708	2755767	3135535

Table S5. The elemental analysis of water soluble bio-oil (WSBO) and water insoluble bio-oil (WIBO). [S5]

	C (mass %)	H (mass %)	O (mass %)	Fraction of total bio-oil
Water soluble bio oil (WSBO)	38.4	52.9	8.7	62%
Water Insoluble bio oil (WSBO)	61	31.5	7.5	38%

This paper should be cited at:
Sharifzadeh M*, Wang L., Shah N., (2015). Decarbonisation of olefin processes using biomass pyrolysis oil. *Applied Energy*, 149, 404–414, (Link).

Table S6. The molar composition of intermediate product streams in the multi-stage catalytic processing (Section 200). [S2]

Compound	CAS number	MW	Formula	mol fraction	mol fraction
				* LT-WSBO	** HT-WSBO
Pentane	109-66-0	72.15	C5H12	0.000	0.004
Hexane	110-54-3	86.18	C6H14	0.000	0.026
Acetic acid	64-19-7	60.05	C2H4O2	0.140	0.070
Levoglucosan	498-07-7	162.14	C6H10O5	0.079	0.000
Sugars ***	4451-30-3	144.12	C6H8O4	0.010	0.001
Methanol	67-56-1	32.04	CH4O	0.068	0.075
Ethanol	64-17-5	46.07	C2H6O	0.014	0.032
1-propanol	71-23-8	60.10	C3H8O	0.004	0.019
Tetrahydrofuran	109-99-9	72.11	C4H8O	0.000	0.002
2-butanol	78-92-2	74.12	C4H10O	0.000	0.005
2-methyltetrahydrofuran	96-47-9	86.13	C5H10O	0.000	0.006
2,5-dimethyltetrahydrofuran	1003-38-9	100.16	C6H12O	0.000	0.004
1-butanol	71-36-3	74.12	C4H10O	0.002	0.004
2-pentanol	6032-29-7	88.15	C5H12O	0.000	0.001
1-pentanol	71-41-0	88.15	C5H12O	0.000	0.002
Ethylene glycol	107-21-1	62.07	C2H6O2	0.343	0.308
Cyclopentanol	96-41-3	86.13	C5H10O	0.003	0.006
2-hexanol	626-93-7	102.17	C6H14O	0.000	0.002
Propylene glycol	57-55-6	76.09	C3H8O2	0.109	0.177
2,3-butanediol	513-85-9	90.12	C4H10O2	0.000	0.012
Cyclohexanol	108-93-0	100.16	C6H12O	0.029	0.011
1,2-butanediol	584-03-2	90.12	C4H10O2	0.011	0.046
Tetrahydrofurfuryl alcohol	97-99-4	102.13	C5H10O2	0.000	0.019
1,4-butanediol	110-63-4	90.12	C4H10O2	0.019	0.023
Γ-butyrolactone	96-48-0	86.09	C4H6O2	0.036	0.037
Γ-valerolactone	108-29-2	100.12	C5H8O2	0.003	0.003
Glycerol	56-81-5	92.09	C3H8O3	0.000	0.022
1,2-cyclohexanediol	1460-57-7	116.16	C6H12O2	0.025	0.024
4-hydroxymethyl-γ-butyrolactone	52813-63-5	116.12	C5H8O3	0.019	0.012
Sorbitol	50-70-4	182.17	C6H14O6	0.089	0.005
3-methylcyclopentanol	18729-48-1	100.16	C6H12O	0.000	0.007
1,2,3-butanetriol	3068-00-6	106.12	C4H10O3	0.000	0.010
1,4-pentanediol	626-95-9	104.15	C5H12O2	0.000	0.006
3-methylcyclohexanol	591-23-1	114.19	C7H14O	0.000	0.006
4-methylcyclohexanol	589-91-3	114.19	C7H14O	0.000	0.004
1,2-hexanediol	6920-22-5	118.17	C6H14O2	0.000	0.006
1,2,6-hexanetriol	106-69-4	134.17	C6H14O3	0.000	0.003

* LT-WSBO represents the products of low temperature hydrogenation (R-201 in Fig. S2)

** HT-WSBO represents the products of high temperature hydrogenation (R-202 in Fig. S2)

*** represented by 1,4:3,6-Dianhydro-α-D-glucopyranose

This paper should be cited at:
Sharifzadeh M*, Wang L., Shah N., (2015). Decarbonisation of olefin processes using biomass pyrolysis oil. *Applied Energy*, 149, 404–414, (Link).

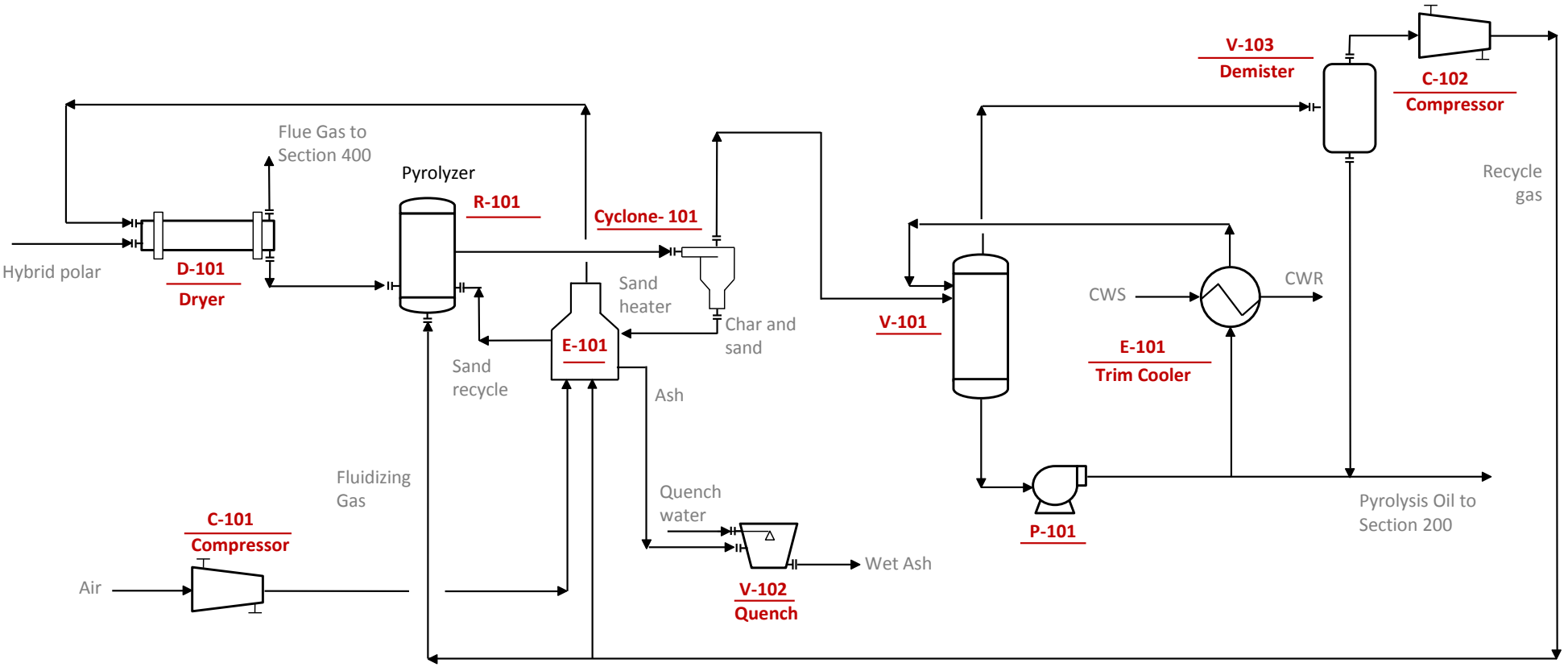

Fig. S1. Biomass pyrolysis (Section 100) - adapted from Jones, *et al.*, [S1]

This paper should be cited at:
Sharifzadeh M*, Wang L., Shah N., (2015). Decarbonisation of olefin processes using biomass pyrolysis oil. *Applied Energy*, 149, 404–414, (Link).

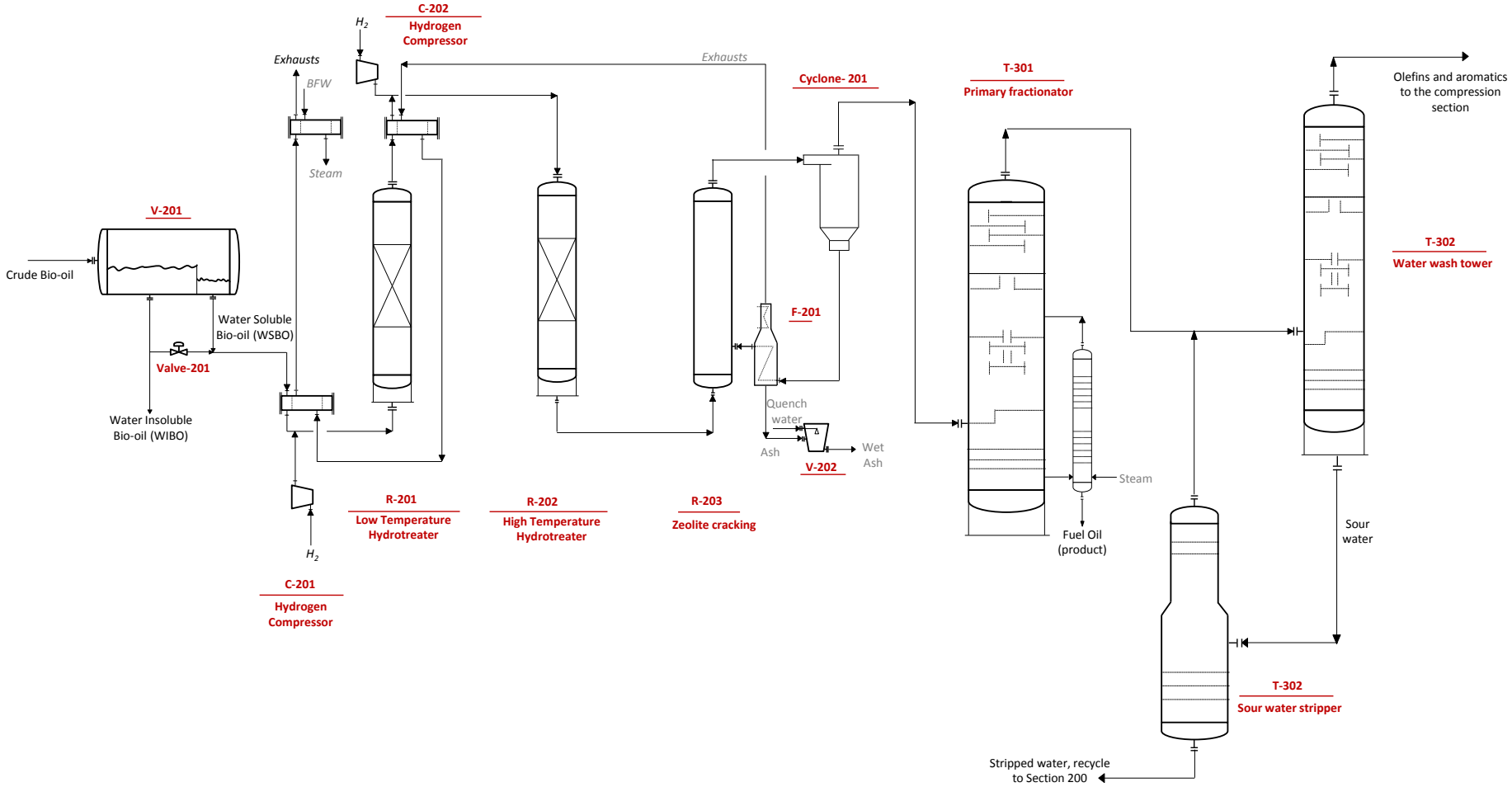

Fig. S2. Bio-oil upgrading (Section 200) and Primary fractionation/ water separation (Section 300)

This paper should be cited at:
Sharifzadeh M*, Wang L., Shah N., (2015). Decarbonisation of olefin processes using biomass pyrolysis oil. *Applied Energy*, 149, 404–414, (Link).

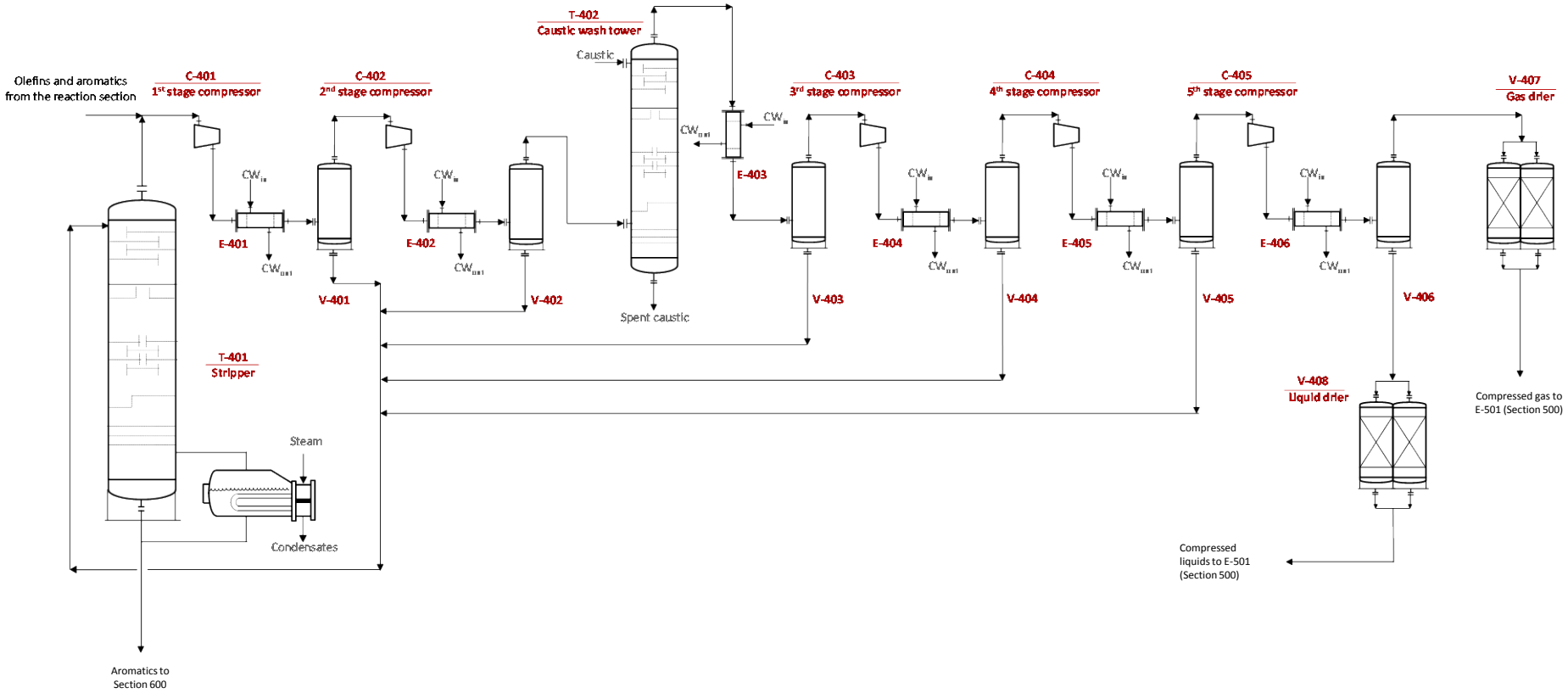

Fig. S3. Energy induced separation network (EISEN) - Section 400

This paper should be cited at:
Sharifzadeh M*, Wang L., Shah N., (2015). Decarbonisation of olefin processes using biomass pyrolysis oil. *Applied Energy*, 149, 404–414, (Link).

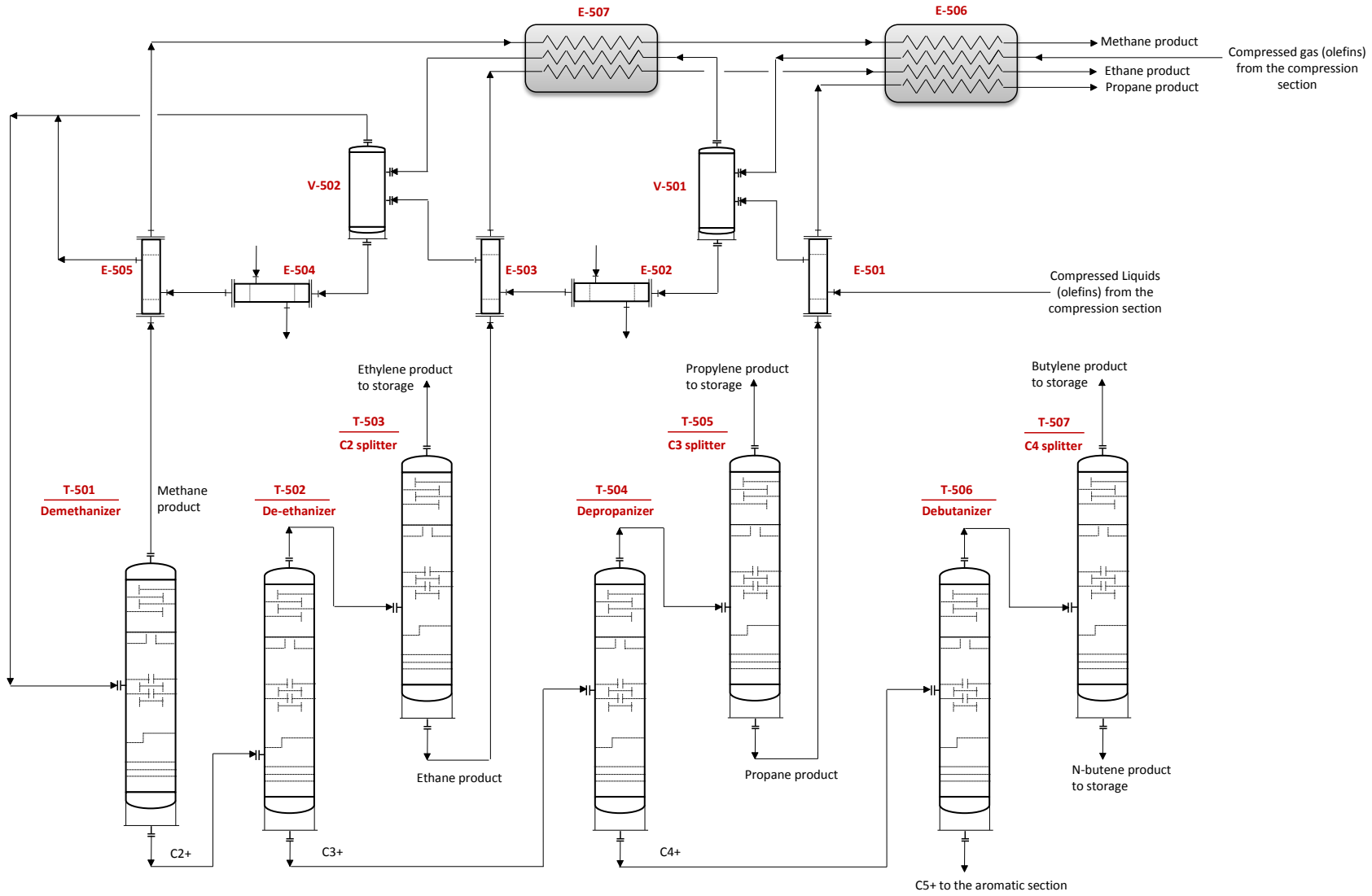

Fig. S4. Cryogenic distillation of olefin products - Section 500

This paper should be cited at:
Sharifzadeh M*, Wang L., Shah N., (2015). Decarbonisation of olefin processes using biomass pyrolysis oil. *Applied Energy*, 149, 404–414, (Link).

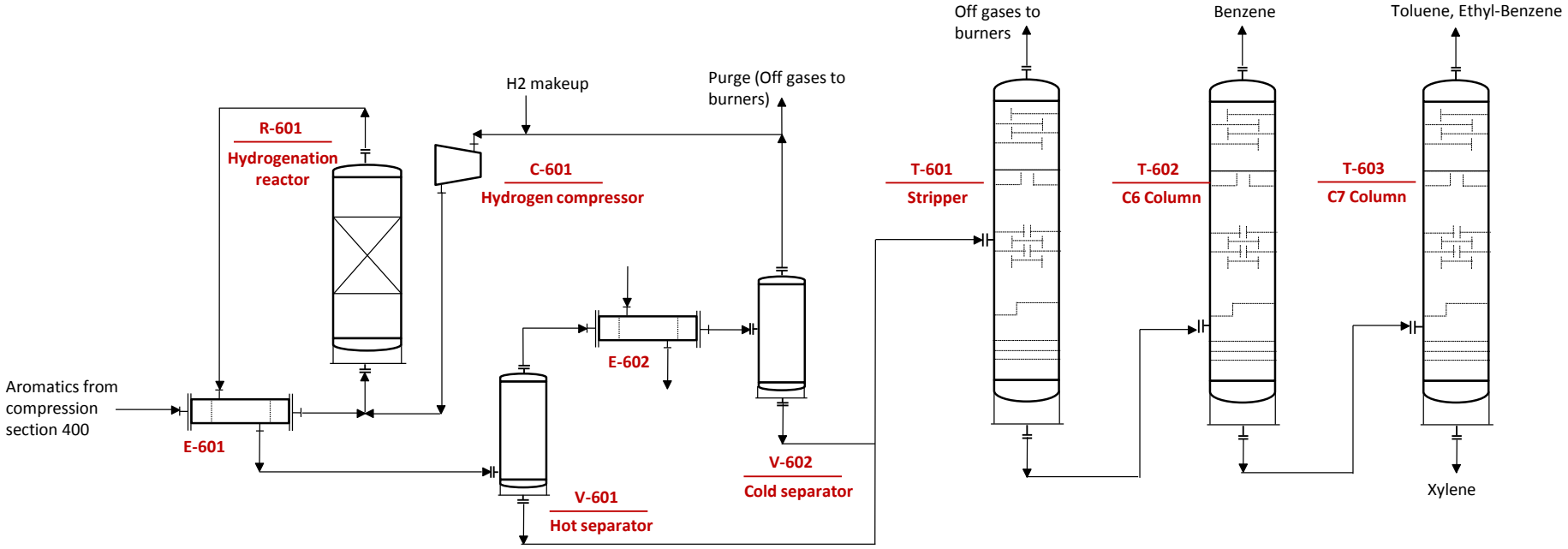

Fig. S5. Pyrolysis oil hydrogenation/Distillation of aromatic - Section 600

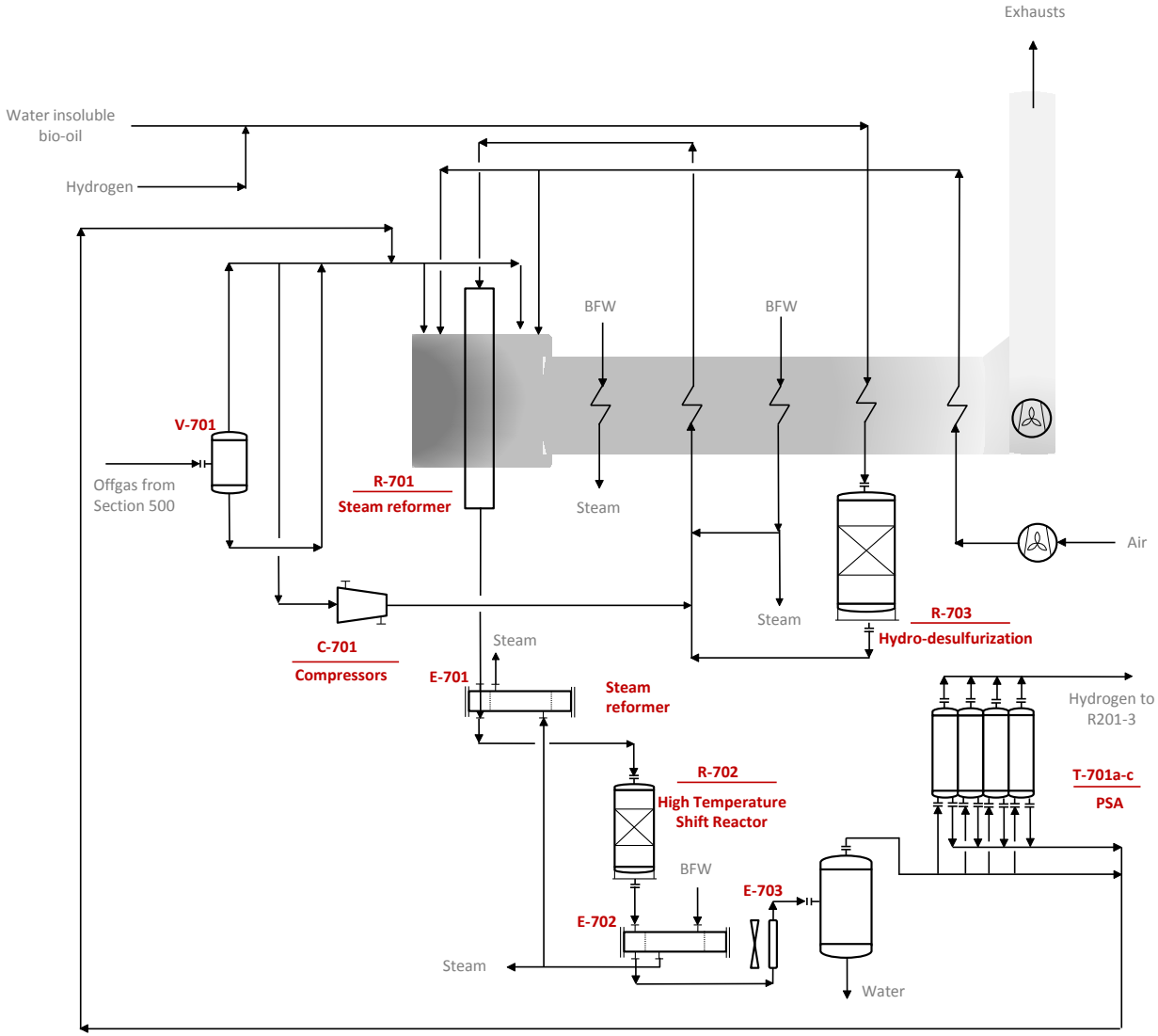

Fig. S6. Hydrogen production, Section 700- adapted from Jones, *et al.*, [S1]